

Review

Multi-Functional Electrospun Nanofibers from Polymer Blends for Scaffold Tissue Engineering

Samerender Nagam Hanumantharao and Smitha Rao * 

Department of Biomedical Engineering, Michigan Technological University, Houghton, MI 49931, USA

* Correspondence: smithar@mtu.edu

Received: 27 May 2019; Accepted: 12 July 2019; Published: 19 July 2019



Abstract: Electrospinning and polymer blending have been the focus of research and the industry for their versatility, scalability, and potential applications across many different fields. In tissue engineering, nanofiber scaffolds composed of natural fibers, synthetic fibers, or a mixture of both have been reported. This review reports recent advances in polymer blended scaffolds for tissue engineering and the fabrication of functional scaffolds by electrospinning. A brief theory of electrospinning and the general setup as well as modifications used are presented. Polymer blends, including blends with natural polymers, synthetic polymers, mixture of natural and synthetic polymers, and nanofiller systems, are discussed in detail and reviewed.

Keywords: electrospinning; nanofibers; tissue scaffold engineering; polymer blending; functional nanofibers

1. Introduction

The field of tissue engineering involves the fabrication of artificial tissues, artificial organs, and tissue regeneration [1]. Scaffolds are used as templates for tissue engineering studies and are composed of decellularized tissue matrices and synthetic or natural polymer constructs [2]. The scaffolds provide mechanical support as well as the physical cues within the microenvironment, aiding cell growth. To enable optimum conditions, it is necessary to mimic the natural microenvironment. This includes the mechanical properties, such as topography, architecture, elasticity, and stiffness, and biochemical factors, such as surface chemistry, growth factors, and cytokines. This need for mimicking the extracellular matrix (ECM) has driven the design of novel biomaterials and fabrication techniques. The readers are encouraged to refer to some of the recent reviews on this topic [3–9].

While several innovative approaches for tissue engineering have been developed within the last decade, electrospinning has continued to be the most commonly used. The advantages of electrospinning are its versatility, flexibility, ability to use different polymer combinations, and ability to upscale easily. Electrospinning is the modification of the electrospraying process where electrostatic fields are used for liquid atomization to form droplets (Figures 1 and 2A). Since mechanical forces are not used for the formation of fibers, it is also known as hydrodynamic jetting. While the effect of electric fields on droplets have been known since the 17th century and was patented in 1900 by J.F. Cooley [10], practical applications were not well developed. In the latter part of the 20th century Doshi and Reneker demonstrated the versatility of the technique by fabricating fibers from organic polymer solutions [11,12]. The typical setup is straightforward and provides flexibility over the fabrication method. Scaling the system for mass manufacturing is relatively easy and all the advantages of the approach translate effectively. The common features of the set-up include a voltage source, syringe pumps, and a collector. For all forms of electrospinning, an initial sol-gel composed of polymers in suitable solvents is needed. The use of one or more polymers with compatible solvents has been reported [13–15].

Polyblending or polymer blending is an effective strategy to blend polymers by incorporating the unique properties of the component polymers or to create novel materials [16]. They can be sub-classified based on their miscibility as homogenous (miscible blend) and heterogenous (immiscible) polymer blends. Miscible blends exhibit a single glass transition temperature while immiscible polymer blends exhibit glass transition temperatures of the individual polymer components. Miscible blends usually form clear solutions, while immiscible blends form cloudy solutions. Furthermore, immiscible blends can have a separation of phases if there is no mechanical stimulus. Polymer blends can be distinguished from block and graft polymers because of the formation of chemical bonds to prepare new polymer systems in the latter. The blending of polymers is typically achieved using approaches such as extrusion, mixing, and injection molding, to make sure the polymers are blended correctly and do not separate out. The thermodynamics of the polymer systems play a major role in determining the miscibility of polymer blends. Some of the parameters that can be modified in order to transition from the preparation of a miscible polymer blend to an immiscible polymer blend are molecular weights of the individual polymer components, solubility of the solvents used for making polymer solutions, temperature, and the ratio of the polymer components in the polymer blend. The major challenge involved in the blending of polymers is that most polymers are thermodynamically immiscible and hence separate out unless stabilized using fillers. It is essential that the blends remain stable in order to create functional materials with the desired properties. The advantage of electrospinning is that functional nanofibers can be fabricated from both miscible and immiscible blends. In this review, we will focus on the fabrication of functional scaffolds through the preparation of novel polymer blends and electrospinning. The modifications made to the electrospinning systems are highlighted. The different polymer blends and the method of fabrication are discussed in detail in the later sections.

2. Electrospinning

2.1. Theory

The generalized setup (Figure 1) consists of a voltage source, syringe pump, nozzle, grounded collector, and syringe. A high electric field is applied (>0.5 kV/cm) to the tip of the nozzle through which a polymer solution of compatible viscosity (200–4000 cP) flows through. A grounded collector is used to collect the fibers. The process of electrospinning revolves around the deformation of the polymer droplet at the tip of the nozzle under the influence of an electric field forming a Taylor cone as seen in Figure 2A [17].

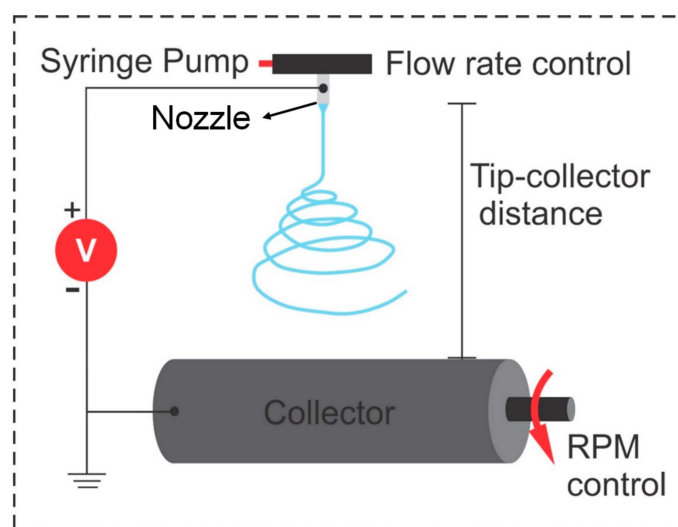


Figure 1. A basic illustration of the electrospinning set-up showing all the possible parameters that can be controlled. Adapted with permission from [18], Samerender Nagam Hanumantharao, 2017.

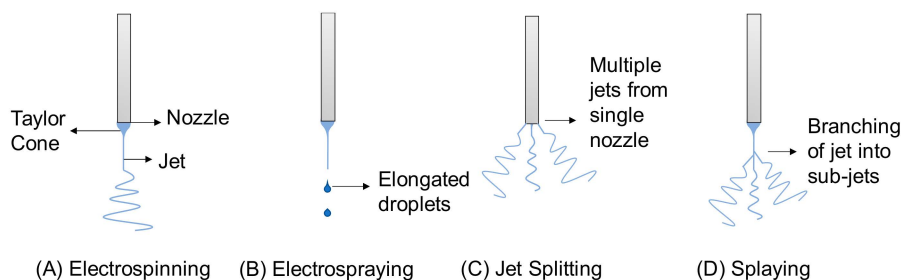


Figure 2. Schematic illustration of the behavior of jets during the electrospinning process.

The entire electrospinning process consists of three stages: Jet initiation, jet elongation, and the formation of nanofibers. The jet initiation starts after the formation of a Taylor cone. The formation of the Taylor cone occurs when the electric field can overcome the surface tension of the polymer solution, thus elongating it. There is a threshold limit to the voltage during which the shape of the Taylor cone changes gradually. A higher voltage causes the droplet to recede into the nozzle while a lower voltage does not create a Taylor cone [19]. The jet travels to the grounded collector or negatively charged collector after ejecting out from the Taylor cone in a linear path initially and later collects on top of it after chaotically moving from the nozzle towards the collector, caused by bending instabilities. The angle of the Taylor cone formed varies depending on the parameters used for electrospinning [20]. The jet initiation process begins when the electric field applied is above the critical voltage value. The critical voltage value is based on the surface tension of the polymer solution and its flow rate. The charge density is highest at the tip of the Taylor cone. Once the jet is initiated, it travels in a linear trajectory. Several parameters play a role in the jet elongation step. Environmental conditions, such as humidity and temperature, electrostatic forces, which are dependent on the electric field applied and the permittivity of the fluid, solvent evaporation rate, and viscoelastic response of the fluid are some of the parameters that affect the process [21].

The acceleration of the jet towards the collector is proportional to the electric field and flow rate. A steady jet is required for continuous electrospinning. The rate of decay of the jet depends on the molecular weight of the polymer and the evaporation rate of the solvent apart from the environmental conditions when the flow rate is constant. A low molecular weight polymer solution or a volatile solvent lead to a faster decay of the jet, leading to splattering or electro spraying (Figure 2B). The forces on the jet vary over time as the jet travels from the tip of the Taylor cone to the collector. Several forces act on the jet in different directions, leading to various fluid instabilities. Splitting of the jet into multiple jets occurs when there is a local charge accumulation on the tip of the jet, leading to branching into sub-jets in a process known as splaying (Figure 2D). Splaying is dependent on the physical and electrical properties of the solvent used and the molecular weight of the polymers. It also generally occurs when a relatively high electric field is used for electrospinning. The process of splaying in different solvents was reviewed in detail by Eda and colleagues [22]. However, in some cases when the electric field applied is higher than the critical value, it leads to receding of the Taylor cone into the nozzle and multiple jets emanating from a single nozzle. This process is known as jet splitting (Figure 2C). After following a linear trajectory, the jet undergoes chaotic flow, which is caused by a non-axisymmetric force or whipping instability [23]. These forces cause the jet to stretch and follow a helical path whose diameter keeps increasing. This provides enough time for the local charges on the tip of the jet to redistribute themselves because of Coulombic repulsion and allows the jet to become elongated and thin. The other instabilities acting on the jet during electrospinning and influencing the formation of nanofibers are the Rayleigh–Plateau instability and an axis-symmetric force. Rayleigh force acts on the jet on opposite sides perpendicular to the surface area of the jet while surface tension works to reduce the total surface area of the jet. This leads to the formation of elongated droplets as the charge on the droplets prevent them from coalescing (Figure 2B). The presence of droplets during electrospinning is not desired in many applications. Hence, a balance between Rayleigh instability and surface tension is needed for continuous electrospinning. The physical properties of the solvent used,

and the viscosity of the polymer solution are key in maintaining the balance [24]. As the jet reaches the collector, it solidifies and forms nanofibers. The electric field applied, solvent used, and polymer concentration play a role in the solidification of the jet and evaporation of the solvents. A process called conglutination, where partially solidified jets lead to the production of fibers that are attached at points of contact, affects the morphology and mechanical properties of the fibers [25]. In the entire process, environmental conditions impact the formation of the Taylor cone, affecting the structure of the nanofibers (diameter, morphology, and mechanical properties). For example, higher humidity leads to the formation of pores on the surface of the nanofibers [26,27]. The entire process of electrospinning can be modified according to the requirements and reengineered to provide more control over the parameters in order to fabricate novel nanostructures. The theoretical models and mechanisms of electrospinning were reviewed in detail by Li et al. [28].

2.2. The Electrospinning Apparatus

The properties of nanofibers that have been fabricated are broadly dependent on the initial sol-gel processing of the polymer blend (e.g., polymer concentration, polarity, solvents used), environmental conditions (humidity and temperature), and parameters used during the electrospinning process (e.g., electric field, polymer flow rate) [29,30]. In this section, the modifications that have been made to the electrospinning apparatus will be discussed. Some of the commonly used configurations are presented here.

2.2.1. Changes in Collector Design

The collector is where the nanofibers are deposited in the process of electrospinning. The basic electrospinning setup consists of a grounded flat surface over which the fibers are collected. Hence, in order to create specific nanostructures, the design of the collector can be modified.

Rotating Mandrel

The rotating mandrel collector consists of a grounded/negatively charged cylinder whose rotation is controlled through an external motor as seen in Figure 1. The use of a rotating mandrel collector helps in the fabrication of aligned nanofibers (Figure 3). The alignment of the fibers is along the direction of the rotation of the collector. The linear rotational velocity of the collector affects the morphology, mechanical strength of the fibers, and crystallinity [31,32]. The alignment of fibers along the rotation of the collector takes place only after reaching a critical value of rotational velocity, which is dependent on the time taken for jet solidification. The electrical field and fluid flow rate are also responsible for the alignment. A higher value of the electric field leads to breaking of the fibers while a higher flow rate of the polymer solution provides less time for the jet to solidify and align along the surface. Interestingly, high rotational speeds yield bands of fibers or overlapping fiber architectures. This was used by Persano et al. to create a three-dimensional mat, which was composed of aligned fibers [33].

Patterned Collector

The use of a patterned collector allows the fabrication of nanofibers with varied morphologies, such as a honeycomb structure or patterns with raised morphologies (Figure 4). The collector used can be of two dissimilar materials with patterns for the selective deposition of nanofibers. The collector can be a conductive or a non-conducting surface. The fabrication of aligned nanofibers were also demonstrated by Dan Li [34]. The surface area and geometry of the collector play a major role in the deposition of fibers. Modeling the electrostatic behavior and altering the polymer solution potentially leads to the fabrication of nanofibers of novel morphologies. Ding et al. demonstrated the deposition of Poly(ethylene oxide) (PEO) fibers on a patterned collector composed of pyramidal protrusions [35]. The fibers were selected and deposited on the tips to form a pattern.

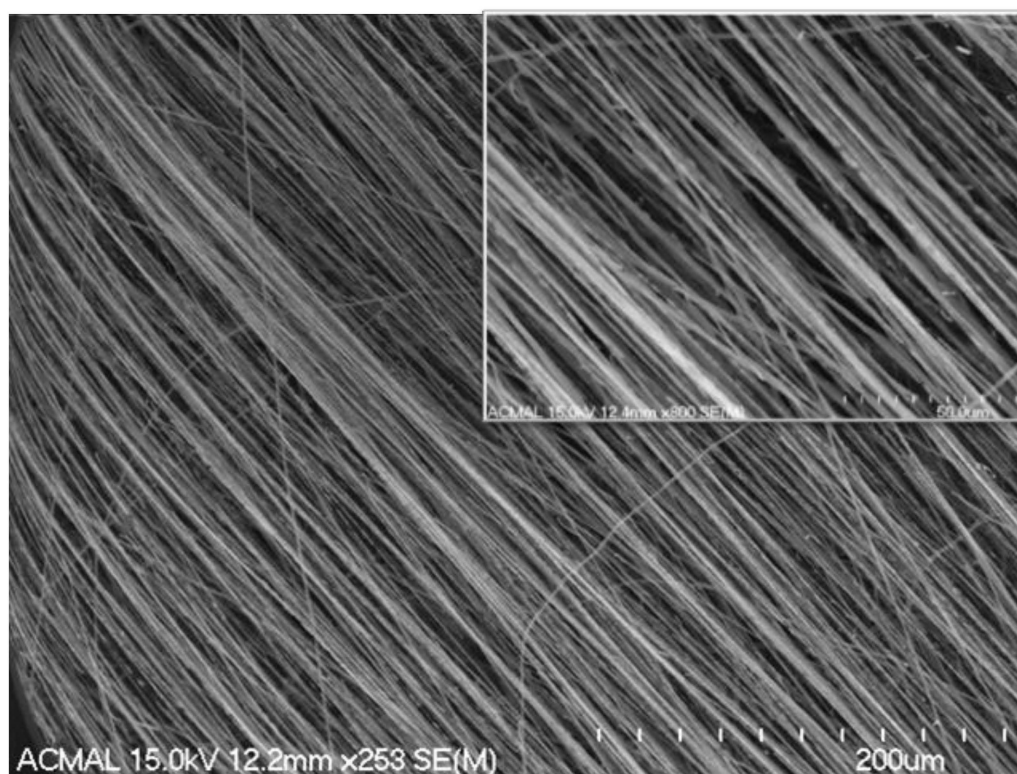


Figure 3. Field Emission Electron Scanning Microscope (FESEM) images of aligned PCL fibers fabricated on a rotating collector. The inset image is a high magnification image showing the alignment and directionality of the fibers. Adapted with permission from [18], Samerender Nagam Hanumantharao, 2017.

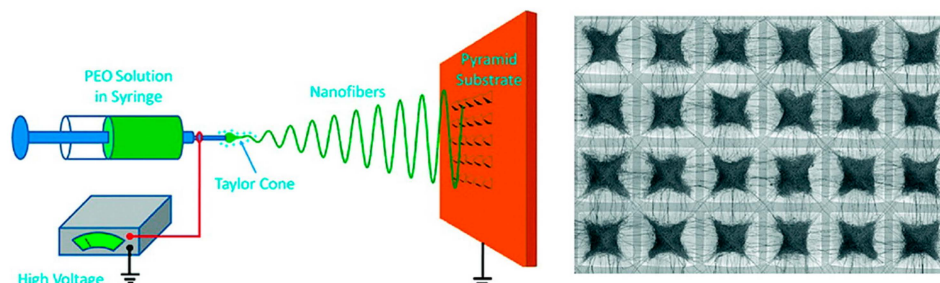


Figure 4. A representation of the electrospinning technique used by Ding and colleagues for the controlled deposition of fibers on a patterned collector. Adapted with permission from [35], American Chemical Society, 2009.

Gap Electrospinning

Gap electrospinning is an alternate way of achieving aligned nanofibers over long distances. A schematic representation of the gap electrospinning setup is shown in Figure 5. The collector consists of two conductive electrodes, which are separated by an insulating gap. The fibers are deposited from one end of the electrodes to the other as the insulating gap causes the fibers to depend on the electrostatic attraction provided by the conductive electrodes. The collector can further be modified with the use of multiple electrodes or stacking electrodes to get thicker 3D constructs.

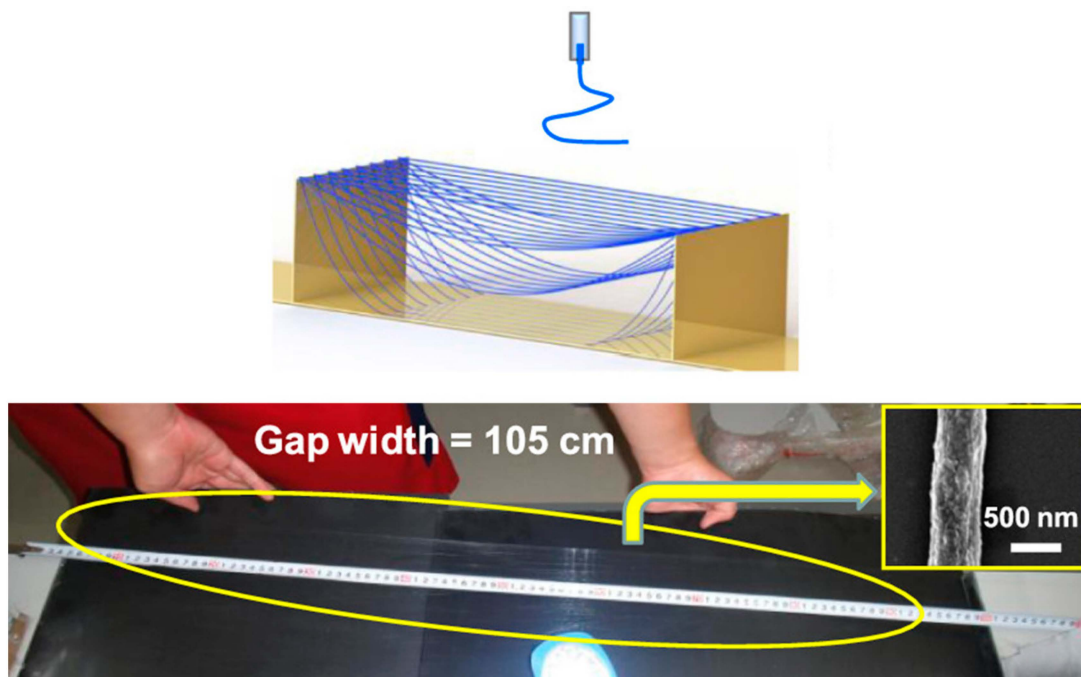


Figure 5. A representation of gap electrospinning and the length of fibers that can be produced by the technique. Adapted with permission from [36], American Chemical Society, 2018.

Magnetic Field Associated Electrospinning

A magnetic field has been used as a parameter to align nanofibers. Polymer solutions are deposited on a collector, which has magnets positioned in parallel, similar to gap electrospinning, to ensure alignment as reported by Yaqing Liu [37]. This technique can be used to stretch the fibers and manipulate the branching of jets to influence the electrical and mechanical properties. The technique introduces an additional force on the jet and can be used to balance out the instabilities caused in the jets.

Wet Spinning

In wet spinning, the electrospun fibers are collected on the surface of a liquid, such as water, which is grounded or negatively charged. In this technique, layers of random fibers are collected, leading to the fabrication of thick constructs. The use of water provides control over the porosity of the scaffold. Tzezana et al. reported the fabrication of 3D constructs for tissue engineering using hydrospinning [38]. The porosity of the scaffold fabricated ensured increased cellular infiltration compared to the fabrication of scaffolds on a plate. The porosity of the electrospun fibers was 80.4% with an average thickness of 0.29 mm while the fibers fabricated through wet spinning had a porosity of 99.3% with an average thickness of 10 mm.

2.2.2. Changes in Orientation

This section discusses the changes that have been made in the geometrical positioning of the tip and collector. The generally used set-up is vertical electrospinning, where gravity acts on the droplet, thereby attracting it to the collector. The alternatives to these arrangements are horizontal electrospinning and converse electrospinning.

Vertical Electrospinning

This is the conventionally used electrospinning set-up, where the spinneret is positioned in parallel on top of a collector (Figure 6A). Gravitational forces act on the jet during electrospinning, accelerating the jet elongation and jet decay. Several studies exist to show the role of parameters

and equations modeling the electrospinning process, generally considering gravitational forces to be constant throughout the process [39–42].

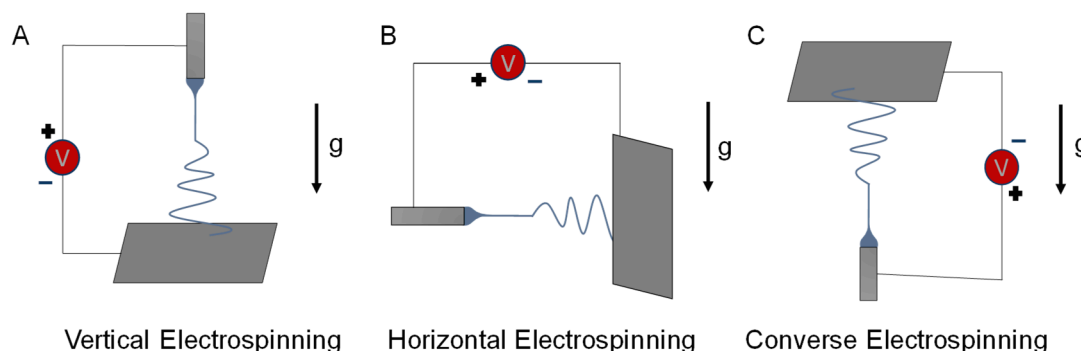


Figure 6. A schematic illustration of the different electrospinning modifications made by changes in orientation of the electrospinning. The effect of gravity causes changes in the resultant nanostructures and affects the electrospinning process.

Horizontal Electrospinning

Horizontal electrospinning is thus called because the electrical fields are parallel to the ground. The spinneret and the collector are along the same axis, parallel to the ground (Figure 6B). The gravitational forces act on the droplet in the downward direction and hence higher electrical fields are needed to overcome the surface tension of the polymer solution and gravitational forces. The projectile motion of the jet is different because of the additional forces and the altered shape of the Taylor cone.

Converse Electrospinning

The converse electrospinning is the converse of the vertical electrospinning method. The spinneret is positioned perpendicular to the ground underneath the collector, which is parallel to the ground (Figure 6C). The spinneret and the collector lie on the same vertical axis. The effect of gravitational force is highest on the droplet and acts against it. Hence, higher electrical fields are required to initiate the formation of a Taylor cone compared to vertical and horizontal electrospinning. Thicker diameter nanofibers with a very narrow size distribution are obtained using this technique [43].

2.2.3. Changes in Spinneret

Coaxial Electrospinning

Coaxial electrospinning is a modification where multiple polymer solutions are electrospun simultaneously from coaxial capillaries to form coaxial or multi-axial nanofibers as seen in Figure 7. The process was first demonstrated by Loscertales and colleagues in 2002, where a coaxial spinneret was used [44]. A schematic representation of the coaxial electrospinning setup and the changes in the Taylor cone during the electrospinning process are shown in Figure 3. The spinneret has two or more separate syringe pumps for the injection of the polymer solutions in the inner and outer capillaries. The inner capillary helps in the formation of the core polymer while the outer capillaries help in the formation of the sheath(es).

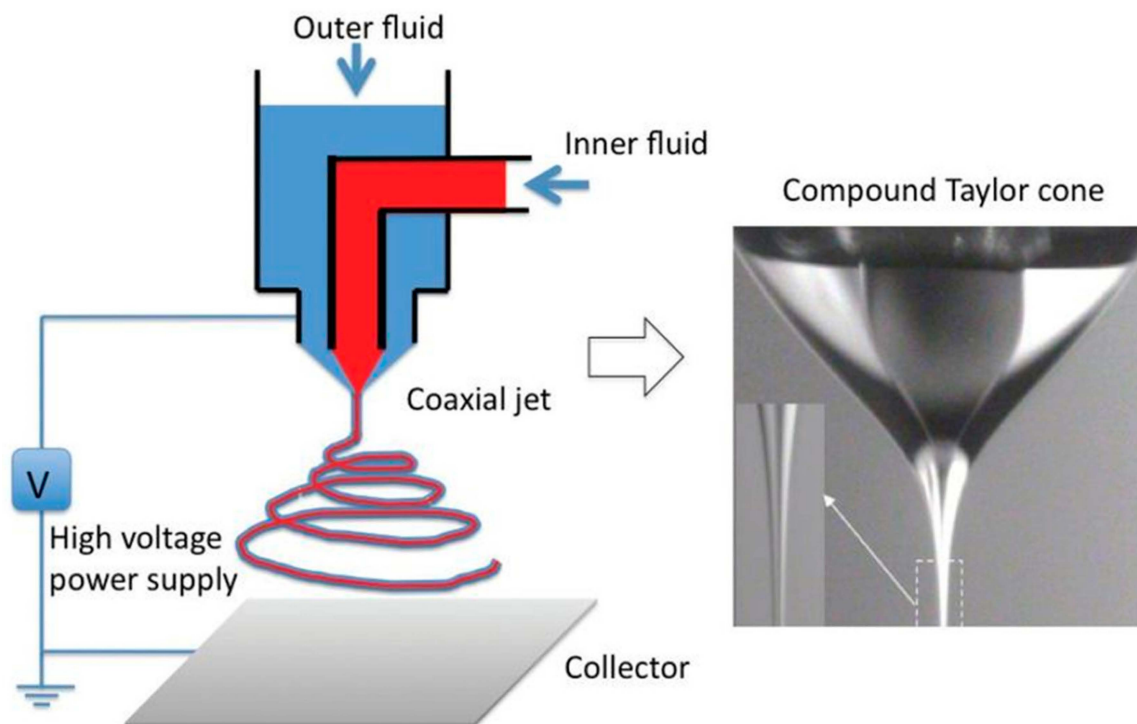


Figure 7. The basic representation of the setup for coaxial electrospinning and the change in the Taylor cone during the fabrication of common core-shell nanofibers. Reprinted with permission from [45], IntechOpen, 2010.

Interestingly, Bazilevsky and colleagues demonstrated the fabrication of coaxial fibers from a single spinneret using selective precipitation of the core polymer in a polymer blend and the polymer present on the sheath was able to form a Taylor cone along with the precipitate as seen in Figure 8 [46]. The theoretical considerations of the formation of coaxial nanofibers using a single nozzle was reviewed in detail by A.L. Yarin [47].

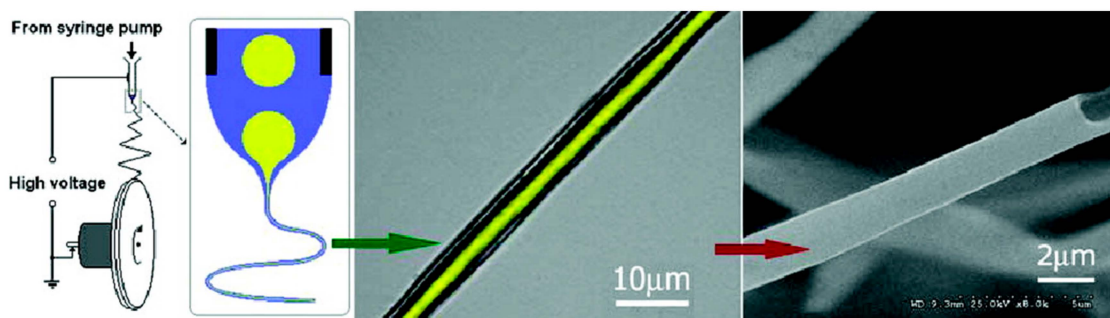


Figure 8. The setup by Bazilevsky and colleagues for the fabrication of single nozzle coaxial electrospinning of polyacrylonitrile (PAN) and poly(methyl methacrylate) (PMMA) using Dimethylformamide (DMF) as a solvent. PAN forms the core while PMMA forms the sheath of the polymer. Reprinted with permission from [46], American Chemical Society, 2007.

Coaxial electrospinning includes a few more controllable parameters than the conventional technique. Since the core and sheath polymers interact, the properties of the polymer solution, like miscibility, boiling point, and viscosity, play a significant role. Additionally, since the process involves electrospinning two or more polymer systems at the same time, the electrospinning parameters need to be compatible. The fluid flow rate is one parameter that can be individually altered during the electrospinning process. Some of the challenges during electrospinning are the solidification of jets

at different points, improper elongation of the jets, and irregular flow rate ratios, which affect the continuous electrospinning process.

Recently, quadriaxial and triaxial spinnerets have also been designed and used to produce tetra-layered and triaxial nanofibers, respectively (Figure 9). The advantage of coaxial electrospinning is that it produces nanofibers of polymers with completely different properties. The core and the sheath polymers retain their properties and, in some cases, enhance the properties of the nanofibers. Also, this technique allows the electrospinning of polymer systems, which are not electrospinnable by themselves due to low viscosity or high conductivity. In order to prepare hollow nanofibers, a sacrificial polymer is used in the core, which is preferentially soluble in a solvent or more thermally degradable than the sheath polymer. Hence, coaxial electrospinning can be used to create novel polymer combinations, such as polymer/inorganic and inorganic/inorganic coaxial nanofibers, and fabrication of nanofibers that contain easily degradable compounds, like enzymes.

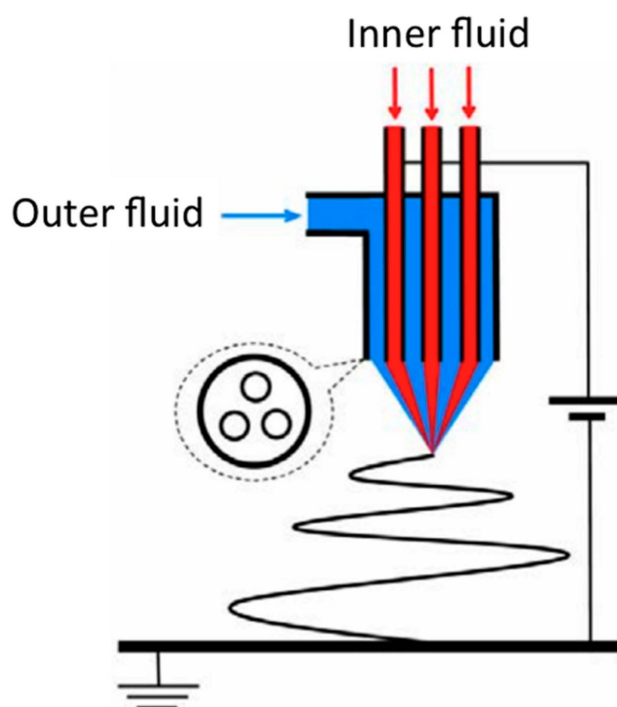


Figure 9. A schematic illustration of an example of a multi-axial spinneret system. Reprinted with permission from [45], IntechOpen, 2010.

Co-Electrospinning

Co-electrospinning involves the use of multiple spinnerets and simultaneous electrospinning on the same collector (Figure 10). This enables the production of composites that have the favorable properties of several polymers. Since different spinnerets are used, the morphologies of the resultant nanocomposites can be varied greatly. Modifications of this technique include using a single voltage source for multiple spinnerets or using multiple spinnerets, each with its own voltage supply. The major challenge associated with co-electrospinning is the interference of the jets during electrospinning. The charges on the jet repel each other and hence, the jets have an angle. While the parameters controlling electrospinning are applicable to co-electrospinning as well, the advantage is in the ability to prepare nanofibers on a large scale using multiple spinnerets. To ensure that there is no interference among the jets, spinnerets placed on either side of the collector to prepare aligned nanofibers have been reported [48]. Co-electrospinning is usually combined with the use of a rotating mandrel to prepare aligned nanocomposites [49].

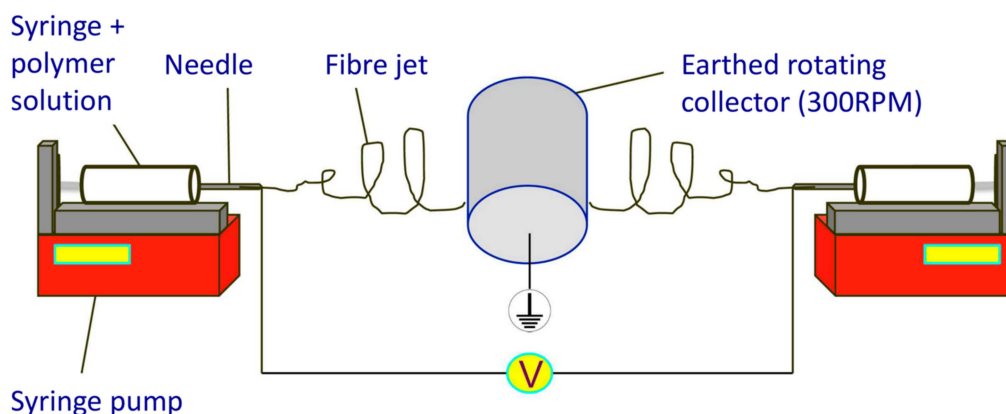


Figure 10. A graphical representation of the co-electrospinning setup used by Hillary and colleagues for the development of scaffolds with improved biophysical properties and bioactivity [50]. Reprinted with permission from [50], PLoS ONE, 2016.

In-Line Polymer Blending

Another approach to create nanocomposites is to combine multiple favorable properties of different polymers for use in in-line polymer blending. The polymer solutions are fed to a mixing chamber and flow through a single spinneret for electrospinning. This method of electrospinning needs precise control of the solvents and polymers used. One of the important advantages of this technique is the fabrication of nanofibers from immiscible and miscible blends, which results in novel nanomaterials.

2.2.4. Other Modifications

Centrifugal Electrospinning

Centrifugal electrospinning uses centrifugal force for the fabrication of nanofibers apart from the electrostatic and gravitational forces. Ultra-thin fibers are produced, owing to the centrifugal forces acting during jet elongation. This technique was first reported by Weitz and colleagues [51]. The set-up consists of a rotating spinneret and an annular collector, which is present around the spinneret. The diameter of the collector is the distance of separation from the tip to the collector. The revolution of the spinneret helps in providing the centrifugal force during electrospinning. This set-up can be further modified by using different spinnerets, like a coaxial spinneret, or co-electrospinning.

Near Field Electrospinning

The design of the setup of near field electrospinning is like the vertical electrospinning set-up, except that the distance between the tip of the spinneret and the collector is in the microscale. The technique is used for the controlled deposition of fibers over a surface. The electric field used is high and the polymer flow rate is maintained to ensure a steady jet. Lin et al. demonstrated the use of near field electrospinning for the production of fibers with diameters ranging from 50 to 500 nm on a collector and the polymer feed rate was similar to that of a dip pen (Figure 11) [52].

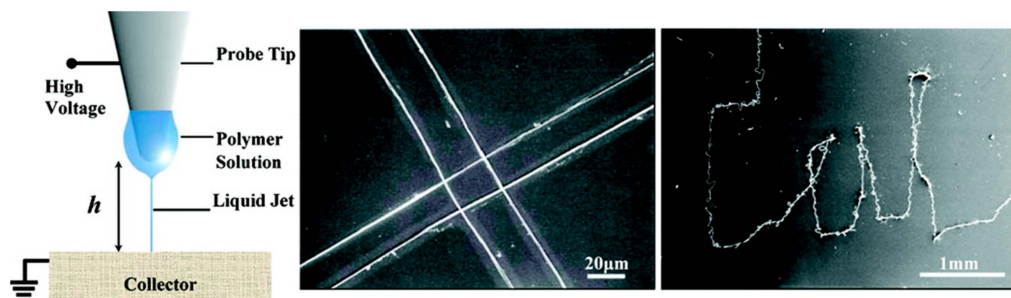


Figure 11. A schematic representation of the near field electrospinning process and the fibers obtained after electrospinning. Sun and colleagues used this technique to demonstrate the fabrication of continuous nanofibers with a desired pattern using a Tungsten tip. Reprinted with permission from [52], American Chemical Society, 2006.

Needleless Electrospinning

The initiation of a jet from a polymer solution can be done if the voltage applied is higher than the critical voltage needed for jet initiation. This theory was used to design spinnerets of any desired shape, a representation of which is shown in Figure 12. The first needle-less electrospinning was demonstrated and patented by Simm et al., where an annular electrode was used as the spinneret [53]. The mode of fiber generation is used to classify the two types of needle-less electrospinning setups. The rotating needle-less electrospinning setup uses mechanical forces to assist in the jet initiation from the surface of the polymer. The jets are formed from a thin layer of polymer solution on the surface of the spinneret because of the mechanical forces. This leads to perturbations assisting in the formation of Taylor cones followed by jet initiation, jet elongation, and fiber formation. Multiple jets are formed from the spinneret. The other mode of needle-less electrospinning is the stationary needle-less electrospinning, where the jet initiation occurs from the liquid surface with the use of external forces, such as magnetic fields, gravity, and the flow of gases. This technique has been in focus recently because of the ease of formation of nanofibers, higher productivity compared to conventional electrospinning, and the advantage of no clogged orifices [54]. The challenge with this technique is the use of a higher voltage for the jet initiation process.

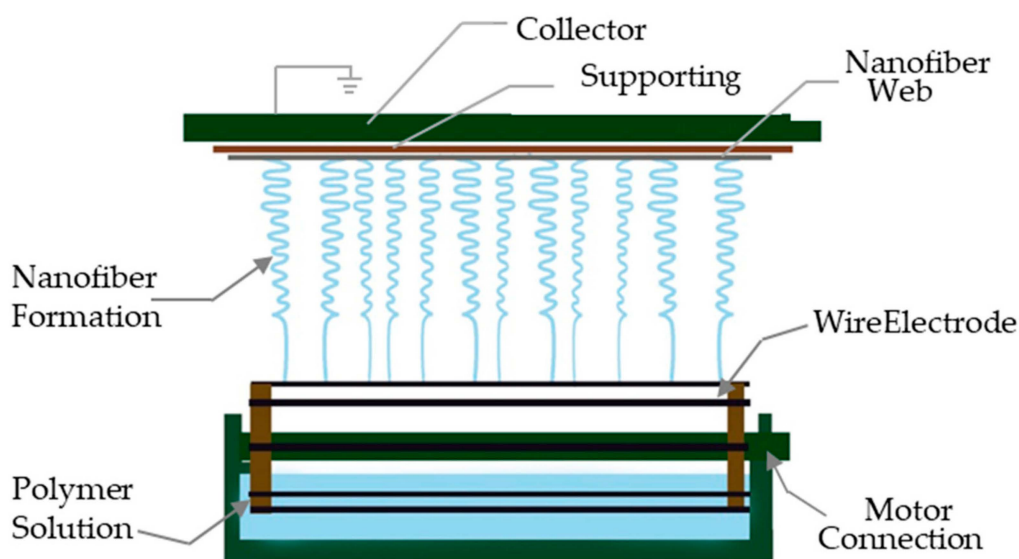


Figure 12. A basic representation of the linear needle-less electrospinning setup [55].

Emulsion Electrospinning

Emulsion electrospinning is a technique used to create nanofibers of different compositions and structures. The feed polymer solution used for electrospinning is an emulsion of two or more polymers that are insoluble with each other. A ratio of hydrophilic and hydrophobic polymers has been used to fabricate fibers with core-shell morphologies as demonstrated by Xu et. al. [56]. Emulsion electrospinning is different from the single nozzle coaxial electrospinning described by Bazilevsky and colleagues [46]. The fibers fabricated using emulsion electrospinning may or may not have a continuous core-shell morphology but are composed of different phases of the polymers. Emulsion electrospinning provides control over the composition of the core and the sheath and diameters of the fibers by allowing modifications of the emulsion composition and the emulsification parameters. This system is beneficial in loading a drug or bioactive component that is soluble only in an inorganic solvent into an organic media or vice versa. The difference in the loading of the component is different compared to polymer blending and coaxial electrospinning as seen in Figure 13. Emulsion electrospinning is advantageous in tissue engineering applications where the bioactive components or drugs can be released in a controlled manner based on the degradation profile of the nanofibers. Some of the model proteins, microRNA, growth factors, and drugs that have been encapsulated are Bovine Serum Albumin (BSA) [57], basic fibroblasts growth factor (bFGF) [58], Cytochrome C [59], doxorubicin hydrochloride (anticancer drug) [60,61], vascular endothelial growth factor (VEGF) and platelet-derived growth factor-bb (PDGF) [62], human-nerve growth factor [63], Rhodamine B [64], microRNA-126 [65], and epidermal growth factor (EGF) [66]. The other major advantage is the use of water-based solvent systems instead of more toxic solvents that provide ease of fabrication and usage.

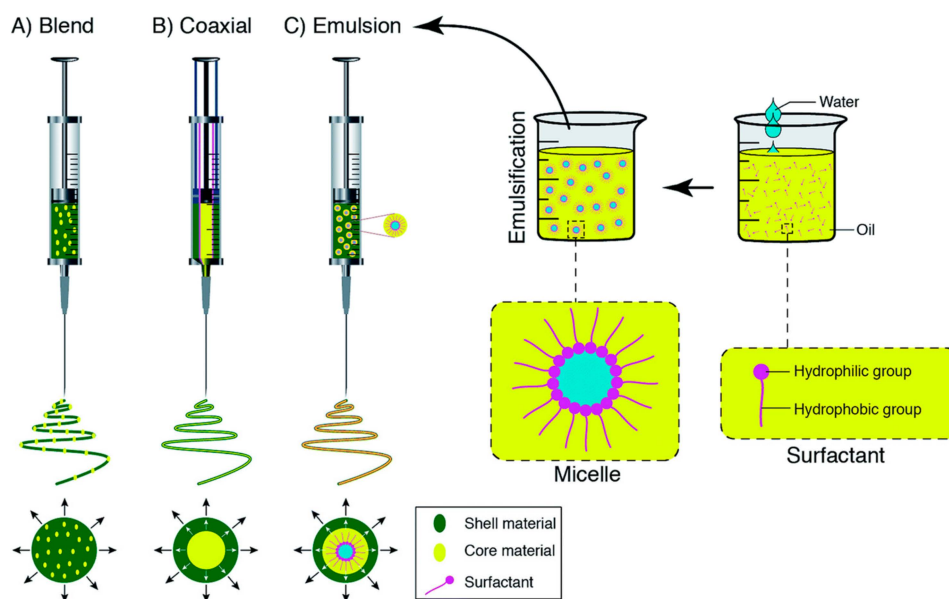


Figure 13. The difference in the loading of the polymer feed solution between blend, coaxial, and emulsion electrospinning and the difference in the resulting structure of the nanofibers. Reprinted with permission from [67], The Royal Society of Chemistry, 2017.

3. Polymer Blends for Tissue Scaffold Engineering

The blends for tissue scaffold engineering are prepared based on the requirements to mimic the extracellular microenvironment. Table 1 summarizes some of the key properties that are used to design an ideal scaffold. Apart from the key properties discussed in the table, properties, such as antibacterial activity, initiating cellular signaling, drug delivery, and electrical conductivity, are useful in scaffolds with more functionality [68–71]. The blends and functional scaffolds are designed and tested based on these design principles. Electrospinning provides flexibility for the formation of

different morphologies of scaffolds. The morphologies of the scaffold play a major role in eliciting an appropriate tissue response and influences stem cell behavior [72–76]. The morphologies of the fibers include the topography of the scaffold and the diameter, orientation, and alignment of the individual nanofibers of the fibrous scaffold.

Table 1. Properties of the scaffold considered when designing a scaffold.

Properties	Design Considerations
Biocompatibility	Ensure scaffolds are compatible with the cells and do not elicit an immune response. An essential requirement of all scaffolds.
Biodegradable/Non-biodegradable	Based on the application, the scaffolds need to be biodegradable or non-biodegradable. Biodegradable scaffolds degrade through enzymatic or hydrolytic action in a controlled manner.
Electrical Conductivity	Electrical signals form an integral part of the cell signaling cascade. Scaffolds that are conductive can be used to manipulate cell behavior accordingly.
Morphology	Cell–scaffold behavior is influenced by the morphology of the scaffold. Porosity is one of the properties that ensures appropriate nutrient transfer to different layers of cells in the scaffold and cellular infiltration. Cellular alignment and migration are also dependent on morphology.
Mechanical Characteristics	Mechanical properties, like the stiffness, Young’s modulus, elasticity, and relaxation modulus, directly affect cell behavior. Mimicking the properties of the scaffold as closely as possible to the natural microenvironment is essential for an ideal scaffold.
Magnetic	Magnetic stimulation in electroactive tissues, like cardiac, nerve, and bone tissues, has shown increased cellular proliferation, differentiation, and cell alignment along the direction of the magnetic field lines. The magnetic field can be applied externally or by using scaffolds which exhibit magnetism.
Bioactivity	Bioactive scaffolds have surface ligands, like Arg-Gly-Asp (RGD) binding sequences, that can be recognized by the host. They elicit a response from the host due to the binding of surface receptors or peptides, or due to the release of degradation products from the scaffold.
Ease of manufacturing	Cost of raw materials, manufacturing process, storage, etc. are some of the factors that influence the effectiveness of a scaffold in tissue engineering applications on a wide scale.

Some of the commonly used morphologies used for tissue engineering applications are scaffolds composed of randomly oriented fibers, aligned fibers, banded fibers, and honeycomb structured fibers (Figure 14). The topographies of each of these morphologies have unique properties that are beneficial in tissue engineering applications. For example, the aligned topography in certain tissues helps in better cellular migration and differentiation [77,78]. The following sections review the developments made in the formation of functional scaffolds through polymer blending and electrospinning. The modifications in electrospinning have been used to fabricate various scaffolds with different morphologies, and structural and chemical properties that are tuned based on the intended application. The chemical properties of the scaffolds are important properties that are tuned in the case of biodegradable or bioabsorbable scaffolds, and to tune the drug release profile from the scaffold. The review by Cheng et al. provides some of the latest innovations in drug delivery from scaffolds by using electrospinning [79]. The state of the art polymer blends used for the fabrication of scaffolds for drug delivery applications were reviewed by Contreras-Cáceres and colleagues [80].

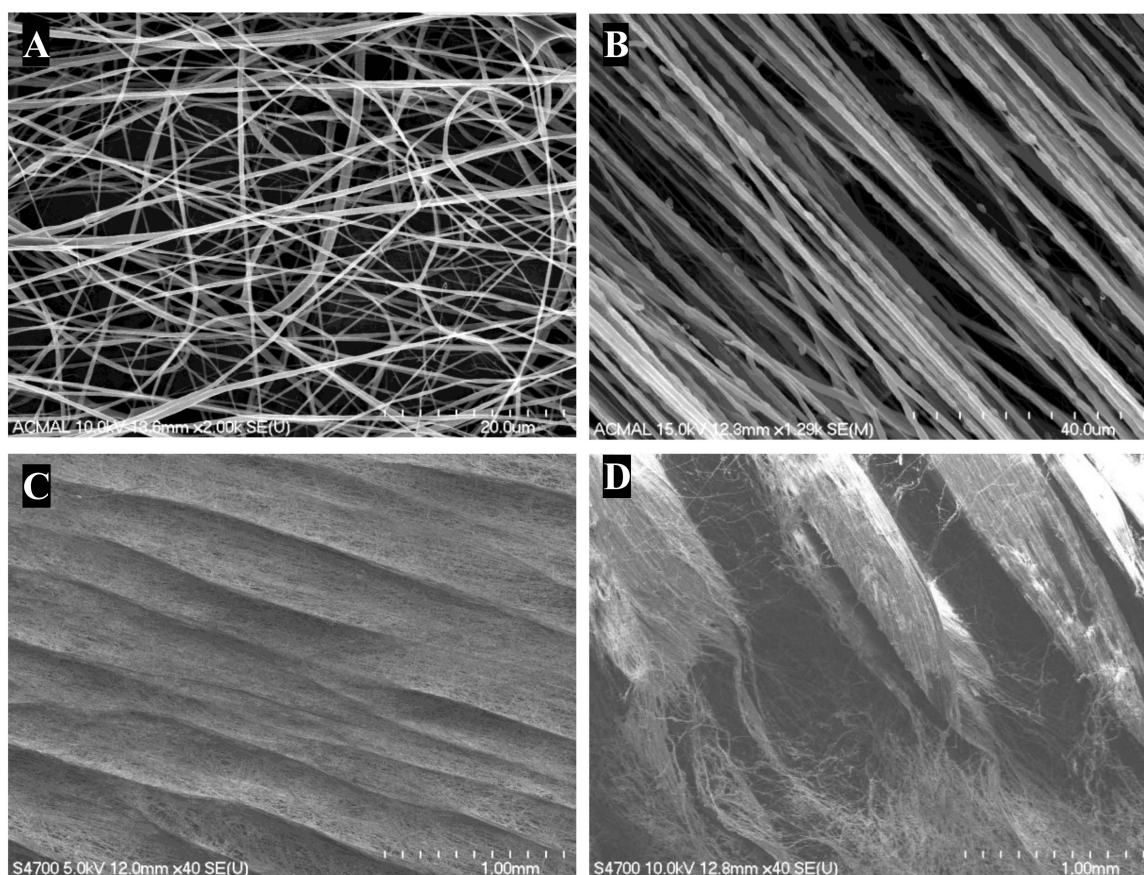


Figure 14. The field emission scanning electron microscope (FESEM) images of the commonly used morphologies for scaffold tissue engineering fabricated using electrospinning. (A) Random morphology composed of randomly oriented fibers (B) The aligned morphology consists of layers of identically oriented fibers in a 3D fibrous structure. (C) Overlapping morphology is composed of layers of fibers overlapped at regions (D) 3D honeycomb structured morphology consists of fibers in a specific arrangement in the scaffold.

3.1. Natural Polymer Blends

Natural polymers are the first choice for the fabrication of scaffolds initially because of their biocompatibility and inherent bioactivity. The commonly used natural polymers in engineering scaffolds are components of the extracellular matrix, like collagen [81], elastin [82], hyaluronic acid [83], and fibrinogen [84], or derivatives from natural sources, like gelatin [85], chitosan [86,87], silk fibroin [88,89], or vegetable oils. The main challenges associated with the use of natural polymers are the strict purification processes, chances of loss in conformation during material processing, difficulty in preparing polymer solutions, variable degradation rates, and lower mechanical strength of the scaffolds. However, polymer blending has been a useful strategy to prepare functional scaffolds that are able to overcome these common problems. The use of post-processing techniques, use of sacrificial templates, and blending with binary or ternary solvent systems has been key to the fabrication of functional scaffolds from natural polymers. Table 2 summarizes the scaffold characteristics in terms of the natural polymers used, solvents used to blend the polymers, modifications to the electrospinning equipment, tissue targeted, and a description of the research.

Table 2. Electrospun scaffolds based on natural polymer blends.

Polymers Used	Solvents Used	Type of Electrospinning	Type of Tissue Engineering	Comments	Ref.
Alginate/Gelatin (PEO: sacrificial template; Pluronic® F-127: Surfactant)	PBS and water	Wet Electrospinning (Ethanol)	Cardiac Tissue Engineering	The method of polymer blending, and choice of electrospinning helped in the formation of a microporous network. The alginate/gelatin hydrogel scaffolds provide a 3D microenvironment which help in maturation of human iPSC-derived ventricular cardiomyocyte.	[90]
Collagen/Chitosan/HA (PEO: Sacrificial template)	Acetic acid, DMSO and water	Vertical Electrospinning	Bone Tissue Engineering	The scaffolds demonstrated osteogenic differentiation and bone regeneration in animal models.	[91]
Gelatin and oxidized carboxymethyl cellulose	Acetic acid and water	Rotating collector coated with PEG	Vascular Tissue Engineering	Scaffolds with tunable mechanical properties and pore sizes were fabricated. The tubular constructs (scaffolds) had a homogenous distribution of fibers.	[92]
Gelatin and Urinary Bladder Matrix	Acetic acid, water and ethyl acetate (Crosslinker: 3 wt% glyoxal)	Low Voltage Electrospinning	-	Biofunctional ECM fibers were fabricated with tunable biochemical, mechanical, and topographical properties.	[93]
Gelatin/Chitosan	TFA and DCM (v/v 7:3)	Vertical Electrospinning	Skin Tissue Engineering	Fibrous scaffolds with improved mechanical properties helped in attachment, migration, and proliferation of cells in vitro.	[94]
Gelatin/Sodium Alginate	Water (CaCl ₂ : crosslinker)	Patterned electrospinning	-	3D printing, freeze drying, and electrospinning were used to manufacture the porous scaffold. Long term in vivo studies demonstrated the ability of cells to vascularize on the scaffolds.	[95]
Gelatin/Glycosaminoglycan	TFE and water	Rotating collector	Cartilage Tissue Engineering	A nanofibrous scaffold was fabricated and tested with stem cells, 15% glycosaminoglycan in gelatin matrix showed the best results.	[96]
HA and collagen (PVP: sacrificial template)	Ethanol	Vertical Electrospinning	Bone Tissue Engineering	Bottom-up method was used to fabricate bone Haversian microstructure scaffold.	[97]
SF and HA (PEO: Sacrificial template)	Water	Wet Electrospinning	Bone Tissue Engineering	Mussel inspired polydopamine was used as an adhesive to coat another layer of HA on the fibers post-electrospinning. The scaffolds promoted cellular differentiation in vitro.	[98]
Zein and Gelatin	Acetic acid/water (v/v 4:1) and 5% w/v glucose	Vertical Electrospinning	-	Maillard reaction was used to crosslink glucose with the proteins. Scaffolds with variable mechanical and surface properties were obtained.	[99]

3.2. Synthetic Polymer Blends

There are a vast number of synthetic polymers that can be used for the fabrication of functional scaffolds. Polymer blending facilitates the incorporation of complementary properties of different synthetic polymers. There are several synthetic polymers that have been approved by the Food and Drug Administration (FDA) for tissue engineering, like PCL [100,101], PLLA, PGA, and PLGA. Some of these polymers are biodegradable while some of the polymers are bioactive because of the degradation products which are recognized by the native tissues. Conductive polymers, such as PANI and PPY [102], and piezoelectric polymers [103], like PVDF, provide additional features to the scaffold and can be used to elicit electrical or mechanical stimulus to the tissues, respectively. The major advantages associated with synthetic polymers are the ease of scaling up, electrospinnability, relative affordability, superior electrical and mechanical characteristics, and relative ease of altering structures. Hanumantharao et al. demonstrated the fabrication of different morphologies of scaffolds from a polymer blend of PCL-PANI using electrospinning as seen in Figure 15. The fibroblasts used for in vitro analysis exhibited a difference in behavior based on morphology [104]. The disadvantage is that following electrospinning, the fibers need to be surface treated before culturing with cells or implantation. Table 3 summarizes the scaffold characteristics in terms of the synthetic polymers used, solvents used to blend the polymers, modifications to the electrospinning equipment, tissue targeted, and a description of the research. The most commonly used polymers as seen from the table are PCL [105], PLLA, and PPY [106].

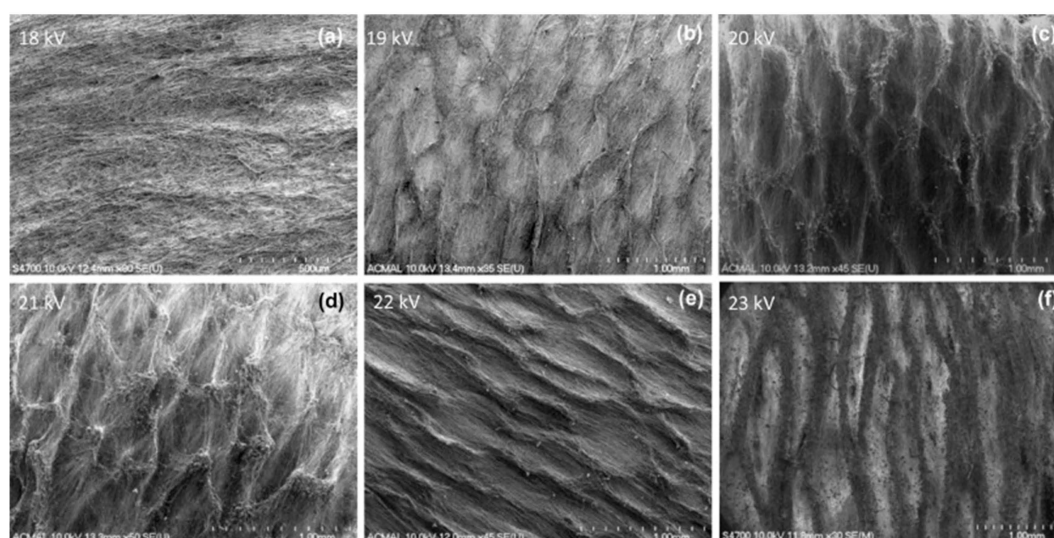


Figure 15. Field Emission Scanning Electron Microscope (FESEM) image of the different morphologies obtained using a synthetic polymer blend of PCL and PANI at different voltages. The scaffolds had no significant change in surface chemistry but had different mechanical properties. Reprinted with permission from [104], Elsevier, 2019.

3.3. Mixed Polymer Blends

Mixed polymer blends are composed of a mixture of natural and synthetic polymers to form a homogenous blend, which is electrospun to fabricate functional scaffolds. The blending and miscibility of synthetic polymers are well characterized because of their relatively known or characterizable glass transition temperatures. Natural polymers have variable glass transition temperatures owing to the variability in processing and changes in conformations. Hence, a blend of natural and synthetic polymer is challenging. A suitable solvent system is needed for preparing the blend, such that the natural polymer does not lose its native structure and consequently, its properties in the blend. Table 4 summarizes the scaffold characteristics in terms of the natural polymers used, synthetic polymers used, solvents used to blend the polymers, modifications to the electrospinning equipment, tissue targeted, and key points of the research.

Table 3. Electrospun scaffolds based on synthetic polymer blends.

Polymers Used	Solvents Used	Type of Electrospinning	Type of Tissue Engineering	Comments	Ref.
PANI, PEG, and PLA	Chloroform, acetone and water	Coaxial and uniaxial electrospinning	Cardiac tissue engineering	Presence of doped PANI and PEG helps in increasing electrical conductivity and affects thermal properties. Use of PLA helps in reducing the toxicity caused by PANI.	[107]
PBAT and PPy	DMF and CF	Climate controlled electrospinning	Bone tissue engineering	The fabricated scaffolds provided a surface for depositing nanohydroxyapatite (nHAp). The scaffolds were bioactive and helped in the differentiation of cells.	[108]
PBAT/PPy	DMF and CF	Vertical Electrospinning	Neural Tissue Engineering	Scaffolds composed of a conductive polymer (PPy) and biodegradable commercial polymer (PBAT) were fabricated through polymer blending and electrospinning. The scaffolds supported neuronal differentiation and spreading.	[109]
PCL (PVA: sacrificial template)	PCL: CF PVA: PC12 cell culture medium	Liquid–liquid coflowing electrospinning method	Neural Tissue Engineering	Fibers with PCL sheath and PVA/PC12 cell cores were fabricated. Cells were grown inside the hollow fibers after dissolving the PVA. The scaffold provides a route to make nerve connections.	[110]
PCL and PANI	HFIP	Vertical Electrospinning	Cardiac Tissue engineering	The fabricated scaffolds provide a conductive 3D environment that showed potential as bio actuators.	[111]
PCL and PANI	Chloroform	Rotating collector	Skin Tissue Engineering	Honeycomb patterns of varying dimensions were fabricated through self-assembly by altering the voltage applied during electrospinning.	[104]
PCL and PGS	CF and acetone	Sequential Electrospinning	Vascular tissue engineering	Tubular scaffolds were fabricated from PGS and PCL. The PGS (inner layer) is a fast degrading polymer that provides a non-thrombogenic surface while PCL (outer layer) provides mechanical stability and controls the degradation rate.	[112]
PCL and PPy	DCM/DMF (v/v 1:1)	Rotating collector	Muscle tissue engineering	Copolymer of PCL-PPy was initially prepared before electrospinning. The scaffolds were conductive and composed of aligned fibers. It was found that conductivity did not play a major role in cellular differentiation.	[113]
PCL or PLLA and hexaaminocyclotriphosphazene (HACTP)	PCL: Formic acid and Acetic acid P LLA: TFA	Needle-less Electrospinning	-	Two different types of scaffolds were fabricated. The addition of HACTP increased the cell spreading, metabolism, proliferation, and bioactivity of the scaffolds.	[114]
PCL/PHB/58S bioactive glass	CF/DMF (v/v 8:2) and ethanol	Horizontal electrospinning	Skeletal tissue engineering	The fabricated fibers exhibited high stiffness of PHB, flexibility of PCL, and bioactivity of 58S bioactive glass.	[115]
PCL/PLGA and BMP-2	PLGA and PCL: TFE BMP-2: BSA and water	Coaxial electrospinning	Bone Tissue Engineering	3D scaffolds were prepared using TISA post-electrospinning. The scaffolds promoted osteogenic differentiation and proliferation.	[116]
PCL/PLGA/PANI	CF/DMF (v/v 3:2)	Rotating collector	Neural Tissue Engineering	Electrically conductive scaffolds were fabricated. The scaffolds when electrically stimulated resulted in neurite outgrowth and cell proliferation in vitro.	[117]
PCL-PLA (4:1)	DCM/DMF (v/v 3:2)	Rotating collector	Bone tissue engineering	Thermally induced nanofiber self-agglomeration (TISA) was used to create 3D nanofibrous scaffolds after the fabrication of electrospun nanofibers. PCL/PLA-3D scaffolds facilitated new bone formation in a cranial bone defect mouse model.	[118]
PHBV/PEO	TFE	Rotating collector electrospinning	Neural Tissue Engineering	The aligned PHBV/PEO fibers after electrospinning were coated with laminin after treatment with plasma. The scaffolds provided topographic cues for the cellular alignment and orientation. In vivo studies demonstrated the effectiveness of the scaffold for peripheral nerve regeneration.	[119]
PU and PGS	Two types of solvent systems were used. CF/DMF (v/v 3:2). HFIP, TFE and acetic acid	Vertical Electrospinning	Vocal fold tissue engineering	Two different solvent systems were used to obtain scaffolds composed of PU/PGS. The morphology and mechanical properties were different when the solvent system was changed. Scaffolds mimicking mechanical properties of vocal folds were fabricated.	[120]
PVA and tetraethyl orthosilicate	Water	Vertical Electrospinning	-	A 3D silica sponge was fabricated using self-assembly. The scaffolds have high porosity, low density, and demonstrated high cell vitality and proliferation rates.	[121]

Table 4. Electrospun scaffolds based on mixture of synthetic and natural polymer blends.

Natural Polymers	Synthetic Polymers	Solvents Used	Type of Electrospinning	Type of Tissue Engineering	Comments	Ref.
6-O-Tritylchitosan (Chitosan derivative)	PCL	DMF	Vertical Electrospinning	Bone Tissue Engineering	The use of chitosan derivative along with PCL helped in increasing the biocompatibility and mechanical properties of the scaffold.	[122]
Alginate/PEO	PCL/PEO	DMSO	Co-electrospinning	Cancer research	Scaffolds with tunable properties were obtained, which interacted with cancer cells differently.	[123]
CA	PVP	Acetone and water	Vertical Electrospinning	Bone Tissue Engineering	Polymer blending and electrospinning was used to create coaxial nanofibers of CA/PVP.	[124]
Carboxymethyl chitosan	PCL	Acetic acid/formic acid (v/v 2:3)	Vertical Electrospinning	Bone Tissue Engineering	Carboxymethyl chitosan was used in place of chitosan to ensure the fabrication of scaffolds with a uniform morphology. The scaffolds promoted cellular proliferation when compared with chitosan/PCL scaffold.	[125]
Chitosan	Polyamide 6,6	Acetic acid and HFIP	Vertical Electrospinning	Bone tissue engineering	The increase in concentration of chitosan showed enhanced suitability as scaffolds by increasing the bioactivity.	[126]
Chitosan	PHB	TFA	Vertical Electrospinning	Cartilage tissue engineering	The blend was prepared to increase the hydrophilicity of the scaffolds.	[127]
Chitosan	PVA	Acetic acid	Needle-less Electrospinning	-	The scaffolds have a controlled degradation rate and mechanical properties.	[128]
Chitosan	PCL	DCM and DMF (v/v 7:3)	Vertical Electrospinning	-	Formation of a 3D scaffold through post-processing of electrospun mats using a needle machine and laminating multiple layers	[129]
Chitosan	PCL	DMF and CF	Rotating collector	-	Nano fibrillated chitosan was blended with PCL to electrospin the scaffolds, resulting in improved mechanical and surface properties compared to PCL.	[130]
Chitosan	PVA	Acetic acid and water	Vertical Electrospinning	-	The nanofibers were crosslinked with glutaraldehyde post electrospinning. The mechanical properties of the scaffolds could be varied by changing the crosslinking time.	[131]
Chitosan	PLA	PLA: CF Chitosan: acetic acid	Vertical Electrospinning	-	A porous nanofiber network of fibers was fabricated using a binary solvent system.	[132]
Chitosan and hyaluronic acid	PCL (PEO: Sacrificial Template)	Water, Formic Acid, Acetones	Vertical Electrospinning	Skin Tissue Engineering	A 3D bilayered scaffold composed of chitosan/PCL-hyaluronic acid was fabricated. The scaffold showed good mechanical and surface properties as well as facilitated cell proliferation and nutrient transfer in comparison to PCL and chitosan/PCL.	[133]
Collagen	PCL and nano bioglass	Acetic acid	Vertical Electrospinning	Nerve Tissue engineering	Bioactive with tunable biodegradation rates were fabricated.	[134]
Collagen	PLA	HFIP and Water (v/v 8:2)	Patterned Electrospinning	Skin Tissue Engineering	Multi-level architecture scaffolds were obtained by using a patterned collector. Collagen helped in improving the mechanical and surface properties of the scaffold.	[135]
Collagen	PLGA	HFIP	Co-electrospinning	Neural Tissue Engineering	The fabricated scaffolds had the advantages of collagen and PLGA. The scaffolds were tested using TBI models on animals and were found to be successful.	[136]
Collagen	PCL	HFIP	Modified Electrospinning setup	Wound healing applications	Manipulation of the collector during fabrication was used to fabricate a nanotopographical patterned scaffold with control over the porosity and pore size.	[137]

Table 4. Cont.

Natural Polymers	Synthetic Polymers	Solvents Used	Type of Electrospinning	Type of Tissue Engineering	Comments	Ref.
Collagen	PCL	HFIP	Near Field Electrospinning	-	Near-field electrospinning was used to create interconnected fiber junctions and fiber overlays.	[138]
Decellularized meniscus extracellular matrix	PCL	HFIP (Crosslinker: 1-ethyl-3-3-dimethylaminopropyl carbodiimide)	Horizontal Electrospinning	Meniscus tissue engineering	In a series of studies, the fabrication of decellularized meniscus extracellular matrix/PCL and their use as scaffolds for meniscus repair were discussed. The scaffold had the surface receptors from the decellularized meniscus extracellular matrix and the tensile strength from PCL. Post-electrospinning, freeze drying, and crosslinking was done to ensure the scaffold mimicked the natural meniscus microenvironment.	[139,140]
Demineralized Bone Matrix and HA	PLGA	PLGA: HFIP; Demineralized Bone Matrix and Sodium hyaluronate: Water	Multi-jet electrospinning with rotating collector	Calvarial defect reconstruction	The scaffolds were fabricated by alternating between electrospinning PLGA and electrospaying demineralized bone matrix and HA on a Mg alloy mesh. The scaffolds provided an attractive treatment option for calvarial defect reconstruction without the use of additional growth factors.	[141]
Fibrinogen and Gelatin	PCL	HFIP and DMEM	Vertical Electrospinning	Neural Tissue Engineering	PCL improved the mechanical properties of the scaffold while gelatin and fibrinogen increased the bioactivity and surface properties of the scaffold. Optimal concentrations of the components in polymer blend were necessary to fabricate the scaffold.	[142]
Gelatin	PGS-PMMA	HFP	Vertical Electrospinning	Nerve tissue engineering	Uniform nanofibers obtained from PGS-PMMA/gelatin blends, which were biocompatible. The PGS-PMMA blend has tunable molecular weights and thermal properties.	[143]
Gelatin	PCL	TFE and acetic acid	Vertical Electrospinning	Endothelium regeneration	Addition of gelatin increased hydrophilicity but decreased mechanical properties. A balance between the two was shown to act as a superior scaffold	[144]
Gelatin	PCL	TFE	Vertical Electrospinning	Vascular Tissue Engineering	Human umbilical vein endothelial cells and adipose-derived mesenchymal stem cells were co-cultured on the PCL/gelatin scaffolds to form blood vessels.	[145]
Gelatin	Poly(ester-urethane) urea	HFIP (Crosslinker: Glutaraldehyde)	Conjugated electrospinning	Skin Tissue Engineering	Nanoyarns were formed using the modified technique of electrospinning. Gelatin helped in increased the wettability of the scaffolds.	[146]
Gelatin	PLLA-CL	HFIP	Conjugated electrospinning with rotating collector	Annulus Fibrosus Tissue Engineering	Aligned nanoyarn scaffolds were fabricated, which have a fibrous 3D morphology and allowed cellular infiltration and proliferation in vivo.	[147]
Gelatin and Aloe Vera extract	PCL	Acetic acid	Co-Electrospinning	Skin Tissue Engineering	The addition of aloe vera extract to the polymer blend during electrospinning helped in increasing fibroblast proliferation compared to PCL and PCL/gelatin scaffolds.	[148]
Gelatin and Chitosan	PGS	Acetic acid	Vertical Electrospinning	Nerve tissue engineering	PGS/chitosan/gelatin (1:1:2) was used to produce nanofibers at the 80 nm scale. Gelatin was incorporated to make the blend homogenous.	[149]
Gelatin and Chondroitin sulfate	PVA	Acetic acid and water	Rotating collector	-	Ternary blend consisting of gelatin, chondroitin sulfate, and PVA was used to fabricate a bead free nanofibrous scaffold.	[150]
Gelatin and HA	PLLA	HFIP	Vertical Electrospinning	Bone Tissue Engineering	Post-processing of electrospun scaffolds was done by homogenizing, freeze-drying, and thermal crosslinking techniques to obtain a 3D scaffold.	[151]

Table 4. Cont.

Natural Polymers	Synthetic Polymers	Solvents Used	Type of Electrospinning	Type of Tissue Engineering	Comments	Ref.
Gelatin and Hyaluronic acid	PLA	HFIP	Vertical Electrospinning	Cartilage Tissue Engineering	A 3D scaffold composed of gelatin/PLA crosslinked with hyaluronic acid was fabricated, which demonstrated enhanced repair of cartilage defects in rabbits.	[152]
Gelatin methacrylamide	PCL	HFIP	Horizontal Electrospinning	Vascular Tissue Engineering	An optimized concentration of polymers in the blend was obtained for appropriate mechanical and surface properties. The scaffolds supported the endothelial cell remodeling by providing the required biological cues and mechanotransduction.	[153]
Gelatin methacrylamide	PCL	HFIP (Ethanol and 2-Hydroxy-4'-(2-hydroxyethoxy)-2-methylpropiophenone used for photocrosslinking)	Co-Electrospinning	Vascular Tissue Engineering	A shape morphing scaffold was manufactured by post-processing the gelatin methacrylamide/PCL fibers and combining it with a shape memory polymer. The scaffold was rolled into 3D tube structures at physiological temperatures. The scaffolds provided an adequate microenvironment for inducing endothelialization.	[154]
HA	PCL	DCM/DMF (v/v 3:2)	Patterned electrospinning	Bone Tissue Engineering	Alternating electrospinning and electro spraying, and a honeycomb patterned collector were used to obtain a scaffold composed of multiple layers of honeycomb patterned PCL nanofibers with HA nanoparticles. In vitro analysis revealed the scaffold promoted osteocompatibility and osteoconduction.	[155]
HA bioceramic	PVA and PCL	PCL and HA bioceramic: CF and Methanol PVA: Water	Co-Electrospinning	Bone Tissue Engineering	The favorable properties of all three components helped in the fabrication of a scaffold that supported the growth of stromal stem cells.	[156]
HSA	PCL	HFIP and water	Electronetting	-	Bimodal structures were obtained in the shape of webs, which help in cell attachment.	[157]
Human Liver ECM proteins	PLLA	HFIP and Acetic acid	Vertical Electrospinning	Liver Tissue Engineering	A translatable niche for hepatocytes was obtained by providing the biochemical cues from the ECM proteins and structural support from PLLA.	[158]
Lactic acid	PCL	DCM/DMF (9:1 ratio by weight)	Multiple pins rotator electrospinning	Connective tissues	Scaffolds mimicking aligned collagen fibrils were fabricated.	[159]
Laminin and Collagen	Polydioxanone	HFIP and water	Magnetic field-assisted electrospinning with coaxial spinneret	Neural Tissue Engineering	Aligned laminin-polydioxanone/collagen core-shell fibers were fabricated. Laminin was systematically released from the fibers. The scaffolds promoted the hippocampal cell behaviors in vitro.	[160]
Lecithin	PLA and PU	THF/DMF mixture	Horizontal electrospinning with rotating collector	Liver Tissue Engineering	The use of PU and lecithin helped in increasing the flexibility, hydrophilicity, and bioactivity. The fibers also had higher hydrophilicity and biocompatibility than the tissue culture plate.	[161]
Lignin	PCL	CF	Vertical Electrospinning	Neural Tissue Engineering	Lignin-PCL copolymers were prepared and blended with PCL and electrospun. The scaffolds displayed free radical scavenging properties and promoted neurite outgrowth and myelin protein expression in Schwann cells.	[162]
Neem oil and Corn oil	PU	DMF	Vertical Electrospinning	Bone Tissue Engineering	Neem oil and corn oil were integrated into the PU matrix to fabricate biocompatible scaffolds with a higher tensile strength and hydrophilicity in relation to PU/corn oil and PU scaffolds.	[163]
Oyster shell	PLLA	CF/DMF (v/v 3:1)	Rotating collector	Bone Tissue Engineering	The scaffolds were composed of aligned fibers. The scaffolds promoted cellular adhesion and differentiation in vivo.	[164]

Table 4. Cont.

Natural Polymers	Synthetic Polymers	Solvents Used	Type of Electrospinning	Type of Tissue Engineering	Comments	Ref.
SF	PU	HFIP	Vertical Electrospinning	Cardiac Tissue Engineering	The scaffolds had variable degradation rates and mechanical properties, which could be controlled by modifying the ratio of SF in the blend. The scaffolds were viable candidates for heart valve tissue engineering.	[165]
SF	PLGA	PLGA: THF and DMF SF: Formic Acid	Multilayer electrospinning	Skin Tissue Engineering	A novel method of electrospinning was used to prepare a sandwich of PLGA between SF. The scaffold fabricated helped in the proliferation of skin cells.	[166]
SF	PEO (sacrificial template)	Ethanol, Water, Formic acid, Calcium chloride	Jet Electrospinning	-	Highly aligned fibers were produced using stable jet electrospinning to form a scaffold with high anisotropy.	[167]
SF	PCL	Formic acid	Wet Electrospinning	Bone Tissue Engineering	Post-processing of the SF/PCL scaffolds was done by functionalizing with polyglutamate acid conjugated with BMP-2 peptide. Wet electrospinning helped in the formation of 3D scaffolds. The functionalized scaffolds enhanced cellular differentiation in comparison with the SF/PCL scaffold.	[168]
SF	PLLA-CL	HFIP	Rotating collector	Bone Tissue Engineering	A dual layered scaffold composed of random and aligned fibers was fabricated. It was found to be a suitable model for tendon to bone healing from in vivo experiments.	[169]
SF	PLLA-CL	HFIP	Vertical Electrospinning	Conjunctiva Reconstruction	Transparent scaffolds were fabricated, which are hydrophilic and porous. Conjunctival epithelial cells were seeded on the scaffolds. The cells seeded on scaffolds were able to form stratified conjunctival epithelium, including goblet cells	[170]
SF	PEO	Water	Vertical Electrospinning	Periodontal tissue regeneration	Ultrasonication was used as a parameter to alter the viscosity of the sol-gel prior to electrospinning. The amount of polymer in the final scaffold could be varied using this technique.	[171]
SF and Platelet-rich plasma	PCL and PVA	HFIP and water	Co-electrospinning	Bone Tissue Engineering	Platelet rich plasma was incorporated into the scaffolds by making a suitable blend with PVA. Co-electrospinning was used to fabricate scaffolds with SF, PCL, PVA, and platelet rich plasma. The scaffolds exhibited a sustained release of platelet rich plasma and promoted cellular differentiation, proliferation, and migration.	[172]
Starch	PVA	Ethanol	Vertical Electrospinning	Wound healing applications	Crosslinking using glutaraldehyde post-electrospinning helped in improving the mechanical properties of the scaffold.	[173]
Sunflower oil and Neem oil	PU	DMF	Vertical Electrospinning	Bone Tissue Engineering	Plant oils were successfully integrated into the polymer matrix to enhance the mechanical properties and bioactivity of the scaffolds.	[174]
Tussah SF	PLA	HFIP	Double conjugate electrospinning [175]	Bone Tissue Engineering	A novel method of electrospinning was used to fabricate scaffolds with high mechanical strength.	[176]
Virgin coconut oil	PU	DMF	Vertical Electrospinning	Vascular Tissue Engineering	The presence of virgin coconut oil in the polymer matrix helped in increasing antithrombogenicity, surface activity, and mechanical properties of the scaffold.	[177]
Zein and Gum Arabic	PCL	Formic acid and glacial acetic acid	Vertical Electrospinning	Skin Tissue Engineering	PCL helped in improving the mechanical properties, zein helped in moderating the degradation while gum arabic helped in improving the surface properties.	[178]

3.4. Nanofiller Polymer Blends

Fillers in polymer blends help to impart specific properties to the fibers. They can be uniformly distributed in the fibers or can be present on the surface. The fillers can aid in the formation of chemical bonds, fill regions in the polymer matrix, change the orientation of polymers, electrical conductivity, and modify surface groups. Table 5 summarizes the scaffold characteristics in terms of the polymers used, fillers used, solvents used to blend the polymers, tissue targeted, and a description of the research. Some of the commonly used nanofillers are HA [179], GO [180], and ferromagnetic nanoparticles [181,182].

Table 5. Electrospun scaffolds based on the use of nanofiller systems.

Polymers Used	Filler	Solvents Used	Type of Tissue Engineering	Comments	Ref.
4-arm PCL-(Zn-curcumin complex) and PVA-carboxymethyl chitosan	GO	DMF and DCM	Bone Tissue Engineering	Core shell nanofibers were fabricated composed of PCL-(Zn-curcumin complex core and GO-PVA-carboxymethyl chitosan sheath. The scaffolds showed enhanced osteogenic capability and antibacterial activity.	[183]
Agarose acetate	β -tricalcium phosphate	Acetic acid and DMAC	Bone Tissue Engineering	The addition of β -tricalcium phosphate helped in increasing cellular differentiation and proliferation in comparison to the scaffold without the filler.	[184]
Alginic acid sodium salt/PVA	Graphene sheets	Water	Neural Tissue Engineering	Electrically conductive scaffolds with high mechanical strength were fabricated. The use of filler helped in increasing the mechanical strength by forming strong bridges with the matrix.	[185]
Chitosan and PU, PPy	Functionalized MWCNT	TFA	Neural Tissue Engineering	Nerve conduit was fabricated using aligned fibers. Post processing of chitosan/PU/MWCNT fibers was done by sheathing with PPy.	[186]
Chitosan/PVP	GO	Acetic acid and distilled water	Skin Tissue engineering	The preparation of chitosan-based blends and addition of GO increased the mechanical properties of the scaffold.	[187]
PCL	ZnO	HFIP	Periodontal tissue engineering	In vivo testing of the scaffolds demonstrated the antibacterial and osteoconductive properties of the fibrous scaffold.	[188]
PCL	Nano HA particles	TFE	Bone Tissue Engineering	A polymer blending method to increase the quantity of nano HA particles were used to fabricate scaffolds.	[189]
PCL and Chitosan (PEO: Sacrificial template)	HA	Acetic acid and DMSO	Tendon and Ligament Regeneration	The HA particles were integrated into the polymer matrix for the fabrication of scaffolds, which are suitable for tendon and ligament regeneration. The scaffolds mimic the mechanical properties closely.	[190]
PCL and Gelatin	halloysite nanotubes	Acetic acid	Wound healing applications	Needle-less and free liquid surface electrospinning was used to fabricate uniform mats. Addition of halloysite nanotubes helped in increasing the mechanical properties of the scaffold.	[191]
PCL/Gelatin	Lanthanum chloride (LaCl ₃)	PCL: DCE and ethanol Gelatin: Formic acid and ethanol	Wound Healing applications	Co-electrospinning using a rotating collector was used for the fabrication of the scaffolds. The scaffolds showed comparable mechanical properties to skin and showed good bioactivity.	[192]
PCL/Gelatin/Chitosan	β -tricalcium phosphate	Acetic acid and Formic acid.	Bone Tissue Engineering	A functional scaffold for guided bone regeneration was fabricated from an immiscible blend. The mechanical and surface properties increased with the increasing concentration of the filler.	[193]
PCL-Aloe Vera	Mg-Ferrite nanoparticles	TFE	-	Magnetic nanofibers were prepared, and in vitro viability was tested on fibroblasts.	[194]
PCL-Chitosan	MgO	TFE and water	-	Fibrous scaffolds with tunable physical properties were fabricated.	[195]
PEA	rGO	CF and DMF	Cardiac Tissue Engineering	The nanofiller decreased the voltage required for electrospinning and increased the electrical conductivity of the scaffolds.	[196]
PHBV	Silicate containing HA	CF	Bone Tissue Engineering	The piezoelectric activity of PHBV and bioactivity of silicate containing HA helped in cellular differentiation, alignment, and proliferation of cells when compared to PHBV scaffolds and PCL scaffolds.	[197]
PLA and Chitosan	Tricalcium Phosphate	TFE	-	Cryomilling was used to prepare a fine powder of the polymers and filler before dissolution. The scaffolds are a suitable candidate for bone tissue engineering application.	[198]
PLA and PVAc	GO	DMF, Chloroform and Acetic acid	Bone Tissue Engineering	The dual-electrospinning technique was used to fabricate triple shaped memory polymers. Addition of GO helped to improve the properties.	[199]
PLGA	GO	HFIP	Skeletal tissue engineering	PLGA and GO (wt. ratio 20:3) were used to create 3D scaffolds with increased hydrophilicity.	[200]

Table 5. Cont.

Polymers Used	Filler	Solvents Used	Type of Tissue Engineering	Comments	Ref.
PLGA	Silica Nanoparticles	HFIP	Bone Tissue Engineering	The scaffolds fabricated promoted cellular differentiation, migration, and proliferation. The mechanical properties of the scaffolds increased as the silica nanoparticles helped to reinforce the fibers.	[201]
PLLA	Fe ₃ O ₄	DCM/DMF (4:1 v/v)	Bone Tissue Engineering	The scaffolds with a filler helped in the better healing of bone defects in animal studies in comparison with neat PLLA grafts.	[202]
PLLA/Lactic acid	β -tricalcium phosphate	DCM/Acetone	Bone Tissue Engineering	Low density fluffy fibrous scaffolds were fabricated. The lactic acid was bleached out post-electrospinning from the scaffolds. The scaffolds promoted cellular infiltration because of their morphology and bioactive filler molecules.	[203]
Poly(3-hydroxybutyrate-co-4-hydroxybutyrate)	GO	CF	Bone Tissue Engineering	The GO in the scaffold helped in modifying the diameter of fibers, positively affecting the mechanical and surface properties of the scaffolds and enhancing cellular differentiation and proliferation in comparison with scaffolds without the filler molecules.	[204]
PU	Zinc Nitrate hexahydrate	DMF	Wound healing applications	The incorporation of zinc nitrate in the PU scaffolds helped in increasing the bioavailability and blood compatibility.	[205]
PU and PDMS	HA nanoparticles	THF	Bone Tissue Engineering	Scaffolds composed of an interconnected pore network were fabricated. The composition of the HA nanoparticles was optimized to ensure maximum cell proliferation and vitality.	[206]
PVA	Nanohydroxy apatite and cellulose nanofibers	Water	Bone Tissue Engineering	The fillers were used to improve the mechanical properties of the scaffold, reduce the degradation rate, and increase cellular activity in relation to PVA/nanohydroxy apatite and PVA fibers.	[207]
PVA	γ -Fe ₂ O ₃	Water	-	The fabrication process involved 3D printing and thermal inversion phase separation for fabrication of the collector and electrospinning of the polymer blend with filler for obtaining the scaffold. The scaffold had milli, micro, and microporous layers because of the fabrication process. The filler helped in increasing the mechanical properties of the scaffold in relation with PVA.	[208]
PVA and Alginate	Graphene (1% PVP dispersing agent)	Water	-	Needle-less electrospinning was used for the fabrication of conductive scaffolds with a high surface area. The inclusion of a filler improved the properties of the scaffold greatly.	[55]
PVDF	Barium Titanate and multiwalled-carbon nanotubes	DMF and Acetone	-	A fluffy 3D fibrous piezoelectric scaffold was fabricated by controlling the relative humidity during electrospinning	[209]
PVDF	GO	DMAC and Acetone	Bone Tissue Engineering	The PVDF containing GO exhibited good osteoconductive properties and can be used as a bioimplant.	[210]
SF	Reduced GO	Formic acid	-	The incorporation of reduced GO in the SF matrix helped improve the mechanical and thermal properties of the scaffold. The scaffolds also promoted osteogenic differentiation in vitro.	[211]
SF	CoFe ₂ O ₄ and Fe ₃ O ₄	Formic acid	-	Magnetic fillers were used to prepare scaffolds, which are magnetically responsive and biodegradable.	[212]
SF	GO	Formic acid	Wound dressing applications	Scaffolds exhibiting antibacterial activity and high porosity were fabricated. GO was integrated into the polymer matrix and this increased the number of oxygen containing groups.	[213]

4. Perspectives and Conclusions

Electrospinning is a relatively old technique but has not yet lost its significance because of its ease of use and ability to be combined with other techniques. The modifications made to the electrospinning apparatus help in adapting the process to fabricate scaffolds with a single polymer or several blended polymers or through multiple inputs. The use of polymer blends adds more flexibility to the manufacturing process. Blends between natural and synthetic polymers and the use of nanofiller systems have been used to demonstrate the fabrication of mechanical, surface, biochemical, and electrical properties, which are impossible to obtain through any single polymer. The blending and electrospinning process has also been used to prepare nanostructures from immiscible blends, which are otherwise unable to be processed. The fabrication of scaffolds that mimic the mechanical,

surface, electrical, and biochemical properties of a variety of tissues have been electrospun and processed. The post-processing of the nanofibers after electrospinning by using techniques such as freeze fracture or cell electrospinning, are interesting methods for further exploration of the potential of electrospinning. Further research is needed to study the dependence on nanotopographical cues in cell behavior in vivo. Techniques, such as rotating collector electrospinning [214] and near field electrospinning [215], have been used previously to fabricate scaffolds that provide topographical cues to the cells in in vitro conditions. New inroads have also been made in the integration of nanofillers and bioactive compounds in the polymer matrix that can induce differentiation, modulate cell behavior, and prevent bacterial infections. The major challenges in the preparation of polymer blends lie in the identification of a suitable solvent system, processing conditions, and method of electrospinning. This is critical for blends containing synthetic and natural polymers, where the window for electrospinning is reduced and the prediction of solubility and miscibility is hard. Finally, the scaffolds fabricated need to be characterized for long-term stability, degradation profiles, and long-term in vivo responses.

Author Contributions: S.N.H., writing—original draft preparation, conceptualization, data curation, methodology, investigation; S.R., project administration, writing—review and editing, supervision.

Funding: This research received no external funding.

Acknowledgments: The authors would like to acknowledge the support received by Samerender Nagam Hanumantharao through the Portage Health Foundation (PHF) graduate assistantship.

Conflicts of Interest: The authors declare no conflict of interest.

Abbreviations

CA	Cellulose Acetate
CF	Chloroform;
DCE	1,2-dichloroethane
DCM	Dichloromethane
DMAC	Dimethylacetamide
DMEM	Dulbecco Modified Eagle's Medium
DMF	N,N-dimethylformamide
DMSO	Dimethyl sulfoxide
ECM	Extracellular Matrix
GO	Graphene Oxide
HA	Hydroxyapatite;
HFP	1,1,1,3,3,3-hexa-fluoro-2-propanol
FESEM	Field Emission Scanning Electron Microscope
HSA	Human Serum Albumin
MWCNT	multiwalled-carbon nanotubes
PANI	Polyaniline
PBAT	Poly(butylene adipate-co-terephthalate)
PBS	Phosphate buffered saline
PCL	Poly-caprolactone
PDMS	polydimethylsiloxane
PEA	Poly(ester amide)
PGA	Polyglycolide
PGS	Poly(Glycerol Sebacate)
PHB	Polyhydroxybutyrate
PHBV	Poly(hydroxybutyrate-cohydroxyvalerate)
PLA	Poly(lactic acid)
PLGA	Poly(lactic-co-glycolic acid)
PLLA	Poly(l-lactic acid)
PLLA-CL	Poly(L-lactic acid-co-e-caprolactone)
PMMA	Poly(methyl methacrylate)
PPy	Polypyrrole

PVA	Polyvinyl alcohol
PVAc	Polyvinyl acetate
PVDF	Polyvinylidene fluoride
PVP	Polyvinyl pyrrolidone
SF	Silk fibroin
TFA	Trifluoroacetic acid
TFE	2,2,2-Trifluoroethanol
TFE	2,2,2-Trifluoroethanol
THF	Tetrahydrofuran

References

- Griffith, L.G.; Naughton, G.J.S. Tissue engineering—Current challenges and expanding opportunities. *Science* **2002**, *295*, 1009–1014. [[CrossRef](#)] [[PubMed](#)]
- Ma, P.X. Scaffolds for tissue fabrication. *Mater. Today* **2004**, *7*, 30–40. [[CrossRef](#)]
- Place, E.S.; Evans, N.D.; Stevens, M.M. Complexity in biomaterials for tissue engineering. *Nat. Mater.* **2009**, *8*, 457–470. [[CrossRef](#)] [[PubMed](#)]
- Chen, F.M.; Liu, X.H. Advancing biomaterials of human origin for tissue engineering. *Prog. Polym. Sci.* **2016**, *53*, 86–168. [[CrossRef](#)] [[PubMed](#)]
- Hinderer, S.; Layland, S.L.; Schenke-Layland, K. ECM and ECM-like materials-Biomaterials for applications in regenerative medicine and cancer therapy. *Adv. Drug Deliv. Rev.* **2016**, *97*, 260–269. [[CrossRef](#)]
- Liu, J.; Sun, L.S.; Xu, W.Y.; Wang, Q.Q.; Yu, S.J.; Sun, J.Z. Current advances and future perspectives of 3D printing natural-derived biopolymers. *Carbohydr. Polym.* **2019**, *207*, 297–316. [[CrossRef](#)] [[PubMed](#)]
- Min, L.L.; Pan, H.; Chen, S.Y.; Wang, C.Y.; Wang, N.; Zhang, J.; Cao, Y.; Chen, X.Y.; Hou, X. Recent progress in bio-inspired electrospun materials. *Compos. Commun.* **2019**, *11*, 12–20. [[CrossRef](#)]
- Bose, S.; Ke, D.X.; Sahasrabudhe, H.; Bandyopadhyay, A. Additive manufacturing of biomaterials. *Prog. Mater. Sci.* **2018**, *93*, 45–111. [[CrossRef](#)]
- Moroni, L.; Boland, T.; Burdick, J.A.; De Maria, C.; Derby, B.; Forgacs, G.; Groll, J.; Li, Q.; Malda, J.; Mironov, V.A.; et al. Biofabrication: A Guide to Technology and Terminology. *Trends Biotechnol.* **2018**, *36*, 384–402. [[CrossRef](#)]
- Cooley, J.F. Improved methods of and apparatus for electrically separating the relatively volatile liquid component from the component of relatively fixed substances of composite fluids. *UK Pat.* **1900**, 6385, 19.
- Doshi, J.; Reneker, D.H. Electrospinning process and applications of electrospun fibers. In Proceedings of the Industry Applications Society Annual Meeting, Toronto, ON, Canada, 2–8 October 1993; pp. 1698–1703.
- Doshi, J.; Reneker, D.H. Electrospinning process and applications of electrospun fibers. *J. Electrostat.* **1995**, *35*, 151–160. [[CrossRef](#)]
- Small, P.A. Some factors affecting the solubility of polymers. *J. Appl. Chem.* **1953**, *3*, 71–80. [[CrossRef](#)]
- Koehn, D.M.; Smolders, C.A. The determination of solubility parameters of solvents and polymers by means of correlations with other physical quantities. *J. Appl. Polym. Sci.* **1975**, *19*, 1163–1179. [[CrossRef](#)]
- Barton, A.F. *CRC Handbook of Solubility Parameters and Other Cohesion Parameters*; Routledge: London, UK, 2017.
- Sionkowska, A. Current research on the blends of natural and synthetic polymers as new biomaterials: Review. *Prog. Polym. Sci.* **2011**, *36*, 1254–1276. [[CrossRef](#)]
- Reneker, D.H.; Yarin, A.L. Electrospinning jets and polymer nanofibers. *Polymer* **2008**, *49*, 2387–2425. [[CrossRef](#)]
- Nagam Hanumantharao, S. A 3D Biomimetic Scaffold Using Electrospinning for Tissue Engineering Applications. Master's Thesis, Michigan Technological University, Houghton, MI, USA, 2017.
- Zargham, S.; Bazgir, S.; Tavakoli, A.; Rashidi, A.S.; Damerchely, R. The Effect of Flow Rate on Morphology and Deposition Area of Electrospun Nylon 6 Nanofiber. *J. Eng. Fibers Fabr.* **2012**, *7*, 42–49. [[CrossRef](#)]
- Yarin, A.L.; Koombhongse, S.; Reneker, D.H. Taylor cone and jetting from liquid droplets in electrospinning of nanofibers. *J. Appl. Phys.* **2001**, *90*, 4836–4846. [[CrossRef](#)]
- Tan, S.H.; Inai, R.; Kotaki, M.; Ramakrishna, S. Systematic parameter study for ultra-fine fiber fabrication via electrospinning process. *Polymer* **2005**, *46*, 6128–6134. [[CrossRef](#)]
- Eda, G.; Liu, J.; Shivkumar, S. Solvent effects on jet evolution during electrospinning of semi-dilute polystyrene solutions. *Eur. Polym. J.* **2007**, *43*, 1154–1167. [[CrossRef](#)]

23. Guerrero, J.; Rivero, J.; Gundabala, V.R.; Perez-Saborid, M.; Fernandez-Nieves, A. Whipping of electrified liquid jets. *Proc. Natl. Acad. Sci. USA* **2014**, *111*, 13763. [\[CrossRef\]](#)
24. Wannatong, L.; Sirivat, A.; Supaphol, P. Effects of solvents on electrospun polymeric fibers: Preliminary study on polystyrene. *Polym. Int.* **2004**, *53*, 1851–1859. [\[CrossRef\]](#)
25. Reneker, D.H.; Kataphinan, W.; Theron, A.; Zussman, E.; Yarin, A.L. Nanofiber garlands of polycaprolactone by electrospinning. *Polymer* **2002**, *43*, 6785–6794. [\[CrossRef\]](#)
26. Pelipenko, J.; Kristl, J.; Janković, B.; Baumgartner, S.; Kocbek, P. The impact of relative humidity during electrospinning on the morphology and mechanical properties of nanofibers. *Int. J. Pharm.* **2013**, *456*, 125–134. [\[CrossRef\]](#)
27. Nezarati, R.M.; Eifert, M.B.; Cosgriff-Hernandez, E. Effects of humidity and solution viscosity on electrospun fiber morphology. *Tissue Eng. Part C Methods* **2013**, *19*, 810–819. [\[CrossRef\]](#)
28. Li, D.; Xia, Y.N. Electrospinning of nanofibers: Reinventing the wheel? *Adv. Mater.* **2004**, *16*, 1151–1170. [\[CrossRef\]](#)
29. Theron, S.A.; Zussman, E.; Yarin, A.L. Experimental investigation of the governing parameters in the electrospinning of polymer solutions. *Polymer* **2004**, *45*, 2017–2030. [\[CrossRef\]](#)
30. Deitzel, J.M.; Kleinmeyer, J.; Harris, D.; Tan, N.C.B. The effect of processing variables on the morphology of electrospun nanofibers and textiles. *Polymer* **2001**, *42*, 261–272. [\[CrossRef\]](#)
31. Kim, K.W.; Lee, K.H.; Khil, M.S.; Ho, Y.S.; Kim, H.Y. The effect of molecular weight and the linear velocity of drum surface on the properties of electrospun poly (ethylene terephthalate) nonwovens. *Fibers Polym.* **2004**, *5*, 122–127. [\[CrossRef\]](#)
32. Baji, A.; Mai, Y.-W.; Wong, S.-C.; Abtahi, M.; Chen, P. Electrospinning of polymer nanofibers: Effects on oriented morphology, structures and tensile properties. *Compos. Sci. Technol.* **2010**, *70*, 703–718. [\[CrossRef\]](#)
33. Persano, L.; Dagdeviren, C.; Su, Y.; Zhang, Y.; Girardo, S.; Pisignano, D.; Huang, Y.; Rogers, J.A. High performance piezoelectric devices based on aligned arrays of nanofibers of poly (vinylidene fluoride-co-trifluoroethylene). *Nat. Commun.* **2013**, *4*, 1633. [\[CrossRef\]](#)
34. Li, D.; Ouyang, G.; McCann, J.T.; Xia, Y. Collecting Electrospun Nanofibers with Patterned Electrodes. *Nano Lett.* **2005**, *5*, 913–916. [\[CrossRef\]](#)
35. Ding, Z.; Salim, A.; Ziaie, B. Selective Nanofiber Deposition through Field-Enhanced Electrospinning. *Langmuir* **2009**, *25*, 9648–9652. [\[CrossRef\]](#)
36. Lei, T.; Xu, Z.; Cai, X.; Xu, L.; Sun, D. New Insight into Gap Electrospinning: Toward Meter-long Aligned Nanofibers. *Langmuir* **2018**, *34*, 13788–13793. [\[CrossRef\]](#)
37. Liu, Y.; Zhang, X.; Xia, Y.; Yang, H. Magnetic-field-assisted electrospinning of aligned straight and wavy polymeric nanofibers. *Adv. Mater.* **2010**, *22*, 2454–2457. [\[CrossRef\]](#)
38. Tzezana, R.; Zussman, E.; Levenberg, S. A Layered Ultra-Porous Scaffold for Tissue Engineering, Created via a Hydrosponning Method. *Tissue Eng. Part C Methods* **2008**, *14*, 281–288. [\[CrossRef\]](#)
39. Spivak, A.F.; Dzenis, Y.A.; Reneker, D.H. A model of steady state jet in the electrospinning process. *Mech. Res. Commun.* **2000**, *27*, 37–42. [\[CrossRef\]](#)
40. Yarin, A.L.; Koombhongse, S.; Reneker, D.H. Bending instability in electrospinning of nanofibers. *J. Appl. Phys.* **2001**, *89*, 3018–3026. [\[CrossRef\]](#)
41. Hohman, M.M.; Shin, M.; Rutledge, G.; Brenner, M.P. Electrospinning and electrically forced jets. II. Applications. *Phys. Fluids* **2001**, *13*, 2221–2236. [\[CrossRef\]](#)
42. Zhao, J.; Si, N.; Xu, L.; Tang, X.; Song, Y.; Sun, Z. Experimental and theoretical study on the electrospinning nanoporous fibers process. *Mater. Chem. Phys.* **2016**, *170*, 294–302. [\[CrossRef\]](#)
43. Yang, C.; Jia, Z.; Xu, Z.; Wang, K.; Guan, Z.; Wang, L. Comparisons of fibers properties between vertical and horizontal type electrospinning systems. In Proceedings of the Electrical Insulation and Dielectric Phenomena, Virginia Beach, VA, USA, 18–21 October 2009; pp. 204–207.
44. Loscertales, I.G.; Barrero, A.; Guerrero, I.; Cortijo, R.; Marquez, M.; Gañán-Calvo, A.M. Micro/Nano Encapsulation via Electrified Coaxial Liquid Jets. *Science* **2002**, *295*, 1695. [\[CrossRef\]](#)
45. Li, F.; Zhao, Y.; Song, Y.L. Core-shell nanofibers: nano channel and capsule by coaxial electrospinning. In *Nanofibers*; Kumar, A., Ed.; IntechOpen: London, UK, 2010; pp. 418–438.
46. Bazilevsky, A.V.; Yarin, A.L.; Megaridis, C.M. Co-electrospinning of Core–Shell Fibers Using a Single-Nozzle Technique. *Langmuir* **2007**, *23*, 2311–2314. [\[CrossRef\]](#)

47. Yarin, A.L. Coaxial electrospinning and emulsion electrospinning of core-shell fibers. *Polym. Adv. Technol.* **2011**, *22*, 310–317. [[CrossRef](#)]
48. Xu, F.; Li, L.; Cui, X. Fabrication of Aligned Side-by-Side TiO₂/SnO₂ Nanofibers via Dual-Opposite-Spinneret Electrospinning. *J. Nanomater.* **2012**, *2012*, 5. [[CrossRef](#)]
49. Xu, W.; Ding, Y.; Huang, R.; Zhu, Z.; Fong, H.; Hou, H. High-performance polyimide nanofibers reinforced polyimide nanocomposite films fabricated by co-electrospinning followed by hot-pressing. *J. Appl. Polym. Sci.* **2018**, *135*, 46849. [[CrossRef](#)]
50. Hillary, C.J.; Roman, S.; Bullock, A.J.; Green, N.H.; Chapple, C.R.; MacNeil, S. Developing Repair Materials for Stress Urinary Incontinence to Withstand Dynamic Distension. *PLoS ONE* **2016**, *11*, e0149971. [[CrossRef](#)]
51. Weitz, R.T.; Harnau, L.; Rauschenbach, S.; Burghard, M.; Kern, K. Polymer nanofibers via nozzle-free centrifugal spinning. *Nano Lett.* **2008**, *8*, 1187–1191. [[CrossRef](#)]
52. Sun, D.; Chang, C.; Li, S.; Lin, L. Near-Field Electrospinning. *Nano Lett.* **2006**, *6*, 839–842. [[CrossRef](#)]
53. Simm, W.; Gosling, C.; Bonart, R.; Falkai, B.V. Fibre Fleece of Electrostatically Spun Fibres and Methods of Making Same. U.S. Patent 4,143,196, 6 March 1979.
54. Yu, M.; Dong, R.H.; Yan, X.; Yu, G.F.; You, M.H.; Ning, X.; Long, Y.Z. Recent Advances in Needleless Electrospinning of Ultrathin Fibers: From Academia to Industrial Production. *Macromol. Mater. Eng.* **2017**, *302*, 19. [[CrossRef](#)]
55. Li, T.-T.; Yan, M.; Xu, W.; Shiu, B.-C.; Lou, C.-W.; Lin, J.-H. Mass-Production and Characterizations of Polyvinyl Alcohol/Sodium Alginate/Graphene Porous Nanofiber Membranes Using Needleless Dynamic Linear Electrospinning. *Polymers* **2018**, *10*, 1167. [[CrossRef](#)]
56. Xu, X.; Zhuang, X.; Chen, X.; Wang, X.; Yang, L.; Jing, X. Preparation of Core-Sheath Composite Nanofibers by Emulsion Electrospinning. *Macromol. Rapid Commun.* **2006**, *27*, 1637–1642. [[CrossRef](#)]
57. Qi, H.X.; Hu, P.; Xu, J.; Wang, A.J. Encapsulation of drug reservoirs in fibers by emulsion electrospinning: Morphology characterization and preliminary release assessment. *Biomacromolecules* **2006**, *7*, 2327–2330. [[CrossRef](#)]
58. Yang, Y.; Xia, T.; Zhi, W.; Wei, L.; Weng, J.; Zhang, C.; Li, X.H. Promotion of skin regeneration in diabetic rats by electrospun core-sheath fibers loaded with basic fibroblast growth factor. *Biomaterials* **2011**, *32*, 4243–4254. [[CrossRef](#)]
59. Maretschek, S.; Greiner, A.; Kissel, T. Electrospun biodegradable nanofiber nonwovens for controlled release of proteins. *J. Control. Release* **2008**, *127*, 180–187. [[CrossRef](#)]
60. Xu, X.L.; Yang, L.X.; Xu, X.Y.; Wang, X.; Chen, X.S.; Liang, Q.Z.; Zeng, J.; Jing, X.B. Ultrafine medicated fibers electrospun from W/O emulsions. *J. Control. Release* **2005**, *108*, 33–42. [[CrossRef](#)]
61. Xu, X.L.; Chen, X.S.; Wang, Z.F.; Jing, X.B. Ultrafine PEG-PLA fibers loaded with both paclitaxel and doxorubicin hydrochloride and their In Vitro cytotoxicity. *Eur. J. Pharm. Biopharm.* **2009**, *72*, 18–25. [[CrossRef](#)]
62. Zhang, H.; Jia, X.L.; Han, F.X.; Zhao, J.; Zhao, Y.H.; Fan, Y.B.; Yuan, X.Y. Dual-delivery of VEGF and PDGF by double-layered electrospun membranes for blood vessel regeneration. *Biomaterials* **2013**, *34*, 2202–2212. [[CrossRef](#)]
63. Li, X.Q.; Su, Y.; Liu, S.P.; Tan, L.J.; Mo, X.M.; Ramakrishna, S. Encapsulation of proteins in poly (L-lactide-co-caprolactone) fibers by emulsion electrospinning. *Colloid Surf. B-Biointerfaces* **2010**, *75*, 418–424. [[CrossRef](#)]
64. Su, Y.; Li, X.Q.; Liu, S.P.; Mo, X.M.; Ramakrishna, S. Controlled release of dual drugs from emulsion electrospun nanofibrous mats. *Colloid Surf. B-Biointerfaces* **2009**, *73*, 376–381. [[CrossRef](#)]
65. Zhou, F.; Jia, X.L.; Yang, Y.; Yang, Q.M.; Gao, C.; Hu, S.L.; Zhao, Y.H.; Fan, Y.B.; Yuan, X.Y. Nanofiber-mediated microRNA-126 delivery to vascular endothelial cells for blood vessel regeneration. *Acta Biomater.* **2016**, *43*, 303–313. [[CrossRef](#)]
66. Wang, Z.B.; Qian, Y.N.; Li, L.H.; Pan, L.H.; Njunge, L.W.; Dong, L.L.; Yang, L. Evaluation of emulsion electrospun polycaprolactone/hyaluronan/epidermal growth factor nanofibrous scaffolds for wound healing. *J. Biomater. Appl.* **2016**, *30*, 686–698. [[CrossRef](#)]
67. Nikmaram, N.; Roohinejad, S.; Hashemi, S.; Koubaa, M.; Barba, F.J.; Abbaspourrad, A.; Greiner, R. Emulsion-based systems for fabrication of electrospun nanofibers: Food, pharmaceutical and biomedical applications. *Rsc Adv.* **2017**, *7*, 28951–28964. [[CrossRef](#)]

68. Chinnappan, A.; Baskar, C.; Baskar, S.; Ratheesh, G.; Ramakrishna, S. An overview of electrospun nanofibers and their application in energy storage, sensors and wearable/flexible electronics. *J. Mater. Chem. C* **2017**, *5*, 12657–12673. [[CrossRef](#)]
69. Timin, A.S.; Muslimov, A.R.; Zyuzin, M.V.; Peltek, O.O.; Karpov, T.E.; Sergeev, I.S.; Dotsenko, A.I.; Goncharenko, A.A.; Yolshin, N.D.; Sinelnik, A.; et al. Multifunctional Scaffolds with Improved Antimicrobial Properties and Osteogenicity Based on Piezoelectric Electrospun Fibers Decorated with Bioactive Composite Microcapsules. *ACS Appl. Mater. Interfaces* **2018**, *10*, 34849–34868. [[CrossRef](#)]
70. Perez, R.A.; Kim, H.-W. Core-shell designed scaffolds for drug delivery and tissue engineering. *Acta Biomater.* **2015**, *21*, 2–19. [[CrossRef](#)]
71. Subbiah, R.; Guldberg, R.E. Materials Science and Design Principles of Growth Factor Delivery Systems in Tissue Engineering and Regenerative Medicine. *Adv. Healthc. Mater.* **2019**, *8*, 1801000. [[CrossRef](#)]
72. Whited, B.M.; Rylander, M.N. The influence of electrospun scaffold topography on endothelial cell morphology, alignment, and adhesion in response to fluid flow. *Biotechnol. Bioeng.* **2014**, *111*, 184–195. [[CrossRef](#)]
73. Ravichandran, R.; Liao, S.; Ng, C.C.; Chan, C.K.; Raghunath, M.; Ramakrishna, S. Effects of nanotopography on stem cell phenotypes. *World J. Stem Cells* **2009**, *1*, 55. [[CrossRef](#)]
74. Kim, D.H.; Lipke, E.A.; Kim, P.; Cheong, R.; Thompson, S.; Delannoy, M.; Suh, K.Y.; Tung, L.; Levchenko, A. Nanoscale cues regulate the structure and function of macroscopic cardiac tissue constructs. *Proc. Natl. Acad. Sci. USA* **2010**, *107*, 565–570. [[CrossRef](#)]
75. Patel, S.; Kurpinski, K.; Quigley, R.; Gao, H.; Hsiao, B.S.; Poo, M.-M.; Li, S. Bioactive nanofibers: Synergistic effects of nanotopography and chemical signaling on cell guidance. *Nano Lett.* **2007**, *7*, 2122–2128. [[CrossRef](#)]
76. Christopherson, G.T.; Song, H.; Mao, H.-Q. The influence of fiber diameter of electrospun substrates on neural stem cell differentiation and proliferation. *Biomaterials* **2009**, *30*, 556–564. [[CrossRef](#)]
77. Chew, S.Y.; Mi, R.; Hoke, A.; Leong, K.W. The effect of the alignment of electrospun fibrous scaffolds on Schwann cell maturation. *Biomaterials* **2008**, *29*, 653–661. [[CrossRef](#)]
78. Ayres, C.; Bowlin, G.L.; Henderson, S.C.; Taylor, L.; Shultz, J.; Alexander, J.; Telemeco, T.A.; Simpson, D.G. Modulation of anisotropy in electrospun tissue-engineering scaffolds: Analysis of fiber alignment by the fast Fourier transform. *Biomaterials* **2006**, *27*, 5524–5534. [[CrossRef](#)]
79. Cheng, H.L.; Yang, X.Y.; Che, X.; Yang, M.S.; Zhai, G.X. Biomedical application and controlled drug release of electrospun fibrous materials. *Mater. Sci. Eng. C-Mater. Biol. Appl.* **2018**, *90*, 750–763. [[CrossRef](#)]
80. Contreras-Cáceres, R.; Cabeza, L.; Perazzoli, G.; Díaz, A.; López-Romero, M.J.; Melguizo, C.; Prados, J. Electrospun Nanofibers: Recent Applications in Drug Delivery and Cancer Therapy. *Nanomater.* **2019**, *9*, 656. [[CrossRef](#)]
81. Fullana, M.J.; Wnek, G.E. Electrospun collagen and its applications in regenerative medicine. *Drug Deliv. Transl. Res.* **2012**, *2*, 313–322. [[CrossRef](#)]
82. Sell, S.A.; Wolfe, P.S.; Garg, K.; McCool, J.M.; Rodriguez, I.A.; Bowlin, G.L. The Use of Natural Polymers in Tissue Engineering: A Focus on Electrospun Extracellular Matrix Analogues. *Polymers* **2010**, *2*, 522–553. [[CrossRef](#)]
83. Campiglio, C.E.; Marcolin, C.; Draghi, L. Electrospun ECM macromolecules as biomimetic scaffold for regenerative medicine: Challenges for preserving conformation and bioactivity. *Aims Mater. Sci.* **2017**, *4*, 638–669. [[CrossRef](#)]
84. Lee, K.Y.; Jeong, L.; Kang, Y.O.; Lee, S.J.; Park, W.H. Electrospinning of polysaccharides for regenerative medicine. *Adv. Drug Deliv. Rev.* **2009**, *61*, 1020–1032. [[CrossRef](#)]
85. Sajkiewicz, P.; Kolbuk, D. Electrospinning of gelatin for tissue engineering-molecular conformation as one of the overlooked problems. *J. Biomater. Sci.-Polym. Ed.* **2014**, *25*, 2009–2022. [[CrossRef](#)]
86. Qasim, S.B.; Zafar, M.S.; Najeel, S.; Khurshid, Z.; Shah, A.H.; Husain, S.; Rehman, I.U. Electrospinning of Chitosan-Based Solutions for Tissue Engineering and Regenerative Medicine. *Int. J. Mol. Sci.* **2018**, *19*, 26. [[CrossRef](#)]
87. Kalantari, K.; Afifi, A.M.; Jahangirian, H.; Webster, T.J. Biomedical applications of chitosan electrospun nanofibers as a green polymer-review. *Carbohydr. Polym.* **2019**, *207*, 588–600. [[CrossRef](#)]
88. Zhang, X.H.; Reagan, M.R.; Kaplan, D.L. Electrospun silk biomaterial scaffolds for regenerative medicine. *Adv. Drug Deliv. Rev.* **2009**, *61*, 988–1006. [[CrossRef](#)]
89. Zhang, J.G.; Mo, X.M. Current research on electrospinning of silk fibroin and its blends with natural and synthetic biodegradable polymers. *Front. Mater. Sci.* **2013**, *7*, 129–142. [[CrossRef](#)]

90. Majidi, S.S.; Slemming-Adamsen, P.; Hanif, M.; Zhang, Z.; Wang, Z.; Chen, M. Wet electrospun alginate/gelatin hydrogel nanofibers for 3D cell culture. *Int. J. Biol. Macromol.* **2018**, *118*, 1648–1654. [\[CrossRef\]](#)
91. Xie, J.; Peng, C.; Zhao, Q.; Wang, X.; Yuan, H.; Yang, L.; Li, K.; Lou, X.; Zhang, Y. Osteogenic differentiation and bone regeneration of iPSC-MSCs supported by a biomimetic nanofibrous scaffold. *Acta Biomater.* **2016**, *29*, 365–379. [\[CrossRef\]](#)
92. Joy, J.; Pereira, J.; Aid-Launais, R.; Pavon-Djavid, G.; Ray, A.R.; Letourneur, D.; Meddahi-Pellé, A.; Gupta, B. Gelatin—Oxidized carboxymethyl cellulose blend based tubular electrospun scaffold for vascular tissue engineering. *Int. J. Biol. Macromol.* **2018**, *107*, 1922–1935. [\[CrossRef\]](#)
93. Li, Z.; Tuffin, J.; Lei, I.M.; Ruggeri, F.S.; Lewis, N.S.; Gill, E.L.; Savin, T.; Huleihel, L.; Badylak, S.F.; Knowles, T.; et al. Solution fibre spinning technique for the fabrication of tuneable decellularised matrix-laden fibres and fibrous micromembranes. *Acta Biomater.* **2018**, *78*, 111–122. [\[CrossRef\]](#)
94. Pezeshki-Modaress, M.; Zandi, M.; Rajabi, S. Tailoring the gelatin/chitosan electrospun scaffold for application in skin tissue engineering: An In Vitro study. *Prog. Biomater.* **2018**, *7*, 207–218. [\[CrossRef\]](#)
95. Chen, H.; Xie, S.; Yang, Y.; Zhang, J.; Zhang, Z. Multiscale regeneration scaffold In Vitro and In Vivo. *J. Biomed. Mater. Res. Part B Appl. Biomater.* **2018**, *106*, 1218–1225. [\[CrossRef\]](#)
96. Honarpardaz, A.; Irani, S.; Pezeshki-Modaress, M.; Zandi, M.; Sadeghi, A. Enhanced chondrogenic differentiation of bone marrow mesenchymal stem cells on gelatin/glycosaminoglycan electrospun nanofibers with different amount of glycosaminoglycan. *J. Biomed. Mater. Res. Part A* **2019**, *107*, 38–48. [\[CrossRef\]](#)
97. Bian, T.; Zhao, K.; Meng, Q.; Tang, Y.; Jiao, H.; Luo, J. The construction and performance of multi-level hierarchical hydroxyapatite (HA)/collagen composite implant based on biomimetic bone Haversian motif. *Mater. Des.* **2019**, *162*, 60–69. [\[CrossRef\]](#)
98. Ko, E.; Lee, J.S.; Kim, H.; Yang, S.Y.; Yang, D.; Yang, K.; Lee, J.; Shin, J.; Yang, H.S.; Ryu, W.; et al. Electrospun Silk Fibroin Nanofibrous Scaffolds with Two-Stage Hydroxyapatite Functionalization for Enhancing the Osteogenic Differentiation of Human Adipose-Derived Mesenchymal Stem Cells. *ACS Appl. Mater. Interfaces* **2018**, *10*, 7614–7625. [\[CrossRef\]](#)
99. Deng, L.; Li, Y.; Feng, F.; Zhang, H. Study on wettability, mechanical property and biocompatibility of electrospun gelatin/zein nanofibers cross-linked by glucose. *Food Hydrocoll.* **2019**, *87*, 1–10. [\[CrossRef\]](#)
100. Cipitria, A.; Skelton, A.; Dargaville, T.R.; Dalton, P.D.; Hutmacher, D.W. Design, fabrication and characterization of PCL electrospun scaffolds—a review. *J. Mater. Chem.* **2011**, *21*, 9419–9453. [\[CrossRef\]](#)
101. Woodruff, M.A.; Hutmacher, D.W. The return of a forgotten polymer—Polycaprolactone in the 21st century. *Prog. Polym. Sci.* **2010**, *35*, 1217–1256. [\[CrossRef\]](#)
102. Guo, B.; Ma, P.X. Conducting polymers for tissue engineering. *Biomacromolecules* **2018**, *19*, 1764–1782. [\[CrossRef\]](#)
103. Rajabi, A.H.; Jaffe, M.; Arinzeh, T.L. Piezoelectric materials for tissue regeneration: A review. *Acta Biomater.* **2015**, *24*, 12–23. [\[CrossRef\]](#)
104. Nagam Hanumantharao, S.; Que, C.; Rao, S. Self-assembly of 3D nanostructures in electrospun polycaprolactone-polyaniline fibers and their application as scaffolds for tissue engineering. *Materialia* **2019**, *6*, 100296. [\[CrossRef\]](#)
105. Malikmammadov, E.; Tanir, T.E.; Kiziltay, A.; Hasirci, V.; Hasirci, N. Polymer Edition. PCL and PCL-based materials in biomedical applications. *J. Biomater. Sci. Polym. Ed.* **2018**, *29*, 863–893. [\[CrossRef\]](#)
106. Huang, Z.B.; Yin, G.F.; Liao, X.M.; Gu, J.W. Conducting polypyrrole in tissue engineering applications. *Front. Mater. Sci.* **2014**, *8*, 39–45. [\[CrossRef\]](#)
107. Bertuoli, P.T.; Ordoño, J.; Armelin, E.; Pérez-Amodio, S.; Baldissera, A.F.; Ferreira, C.A.; Puiggali, J.; Engel, E.; del Valle, L.J.; Alemán, C. Electrospun Conducting and Biocompatible Uniaxial and Core-Shell Fibers Having Poly (lactic acid), Poly (ethylene glycol), and Polyaniline for Cardiac Tissue Engineering. *ACS Omega* **2019**, *4*, 3660–3672. [\[CrossRef\]](#)
108. De Castro, J.G.; Rodrigues, B.V.M.; Ricci, R.; Costa, M.M.; Ribeiro, A.F.C.; Marciano, F.R.; Lobo, A.O. Designing a novel nanocomposite for bone tissue engineering using electrospun conductive PBAT/polypyrrole as a scaffold to direct nanohydroxyapatite electrodeposition. *RSC Adv.* **2016**, *6*, 32615–32623. [\[CrossRef\]](#)
109. Granato, A.E.C.; Ribeiro, A.C.; Marciano, F.R.; Rodrigues, B.V.M.; Lobo, A.O.; Porcionatto, M. Polypyrrole increases branching and neurite extension by Neuro2A cells on PBAT ultrathin fibers. *Nanomed. Nanotechnol. Biol. Med.* **2018**, *14*, 1753–1763. [\[CrossRef\]](#)
110. Wu, Y.; Ranjan, V.D.; Zhang, Y. A Living 3D In Vitro Neuronal Network Cultured inside Hollow Electrospun Microfibers. *Adv. Biosyst.* **2018**, *2*, 1700218. [\[CrossRef\]](#)

111. Wang, L.; Wu, Y.B.; Hu, T.L.; Guo, B.L.; Ma, P.X. Electrospun conductive nanofibrous scaffolds for engineering cardiac tissue and 3D bioactuators. *Acta Biomater.* **2017**, *59*, 68–81. [[CrossRef](#)]
112. Kharazi, A.Z.; Atari, M.; Vatankhah, E.; Javanmard, S.H. A nanofibrous bilayered scaffold for tissue engineering of small-diameter blood vessels. *Polym. Adv. Technol.* **2018**, *29*, 3151–3158. [[CrossRef](#)]
113. Browe, D.; Freeman, J. Optimizing C2C12 myoblast differentiation using polycaprolactone–Polypyrrole copolymer scaffolds. *J. Biomed. Mater. Res. Part A* **2019**, *107*, 220–231. [[CrossRef](#)]
114. Sedláková, V.; Voráč, Z.; Jaroš, J.; Bačovská, R.; Kloučková, M.; Svoboda, M.; Streit, L.; Dumková, J.; Vašíčková, K.; Alberti, M.; et al. Enhanced bioactivity of electrospun PCL and PLLA scaffolds blended with amino-phosphazene. *Mater. Lett.* **2018**, *228*, 339–343. [[CrossRef](#)]
115. Ding, Y.; Li, W.; Müller, T.; Schubert, D.W.; Boccaccini, A.R.; Yao, Q.; Roether, J.A. Electrospun Polyhydroxybutyrate/Poly (ϵ -caprolactone)/58S Sol–Gel Bioactive Glass Hybrid Scaffolds with Highly Improved Osteogenic Potential for Bone Tissue Engineering. *Acs Appl. Mater. Interfaces* **2016**, *8*, 17098–17108. [[CrossRef](#)]
116. Hu, S.; Chen, H.; Zhou, X.; Chen, G.; Hu, K.; Cheng, Y.; Wang, L.; Zhang, F. Thermally induced self-agglomeration 3D scaffolds with BMP-2-loaded core-shell fibers for enhanced osteogenic differentiation of rat adipose-derived stem cells. *Int. J. Nanomed.* **2018**, *13*, 4145–4155. [[CrossRef](#)]
117. Farkhondehnia, H.; Amani Tehran, M.; Zamani, F. Fabrication of Biocompatible PLGA/PCL/PANI Nanofibrous Scaffolds with Electrical Excitability. *Fibers Polym.* **2018**, *19*, 1813–1819. [[CrossRef](#)]
118. Yao, Q.; Cosme, J.G.L.; Xu, T.; Miszuk, J.M.; Picciani, P.H.S.; Fong, H.; Sun, H. Three dimensional electrospun PCL/PLA blend nanofibrous scaffolds with significantly improved stem cells osteogenic differentiation and cranial bone formation. *Biomaterials* **2017**, *115*, 115–127. [[CrossRef](#)]
119. Zhang, X.-F.; Liu, H.-X.; Ortiz, L.S.; Xiao, Z.-D.; Huang, N.-P. Laminin-modified and aligned poly (3-hydroxybutyrate-co-3-hydroxyvalerate)/polyethylene oxide nanofibrous nerve conduits promote peripheral nerve regeneration. *J. Tissue Eng. Regen. Med.* **2018**, *12*, e627–e636. [[CrossRef](#)]
120. Jiang, L.; Jiang, Y.; Stiadle, J.; Wang, X.; Wang, L.; Li, Q.; Shen, C.; Thibeault, S.L.; Turng, L.-S. Electrospun nanofibrous thermoplastic polyurethane/poly (glycerol sebacate) hybrid scaffolds for vocal fold tissue engineering applications. *Mater. Sci. Eng. C* **2019**, *94*, 740–749. [[CrossRef](#)]
121. Mi, H.-Y.; Jing, X.; Napiwocki, B.N.; Li, Z.-T.; Turng, L.-S.; Huang, H.-X. Fabrication of fibrous silica sponges by self-assembly electrospinning and their application in tissue engineering for three-dimensional tissue regeneration. *Chem. Eng. J.* **2018**, *331*, 652–662. [[CrossRef](#)]
122. Seethalakshmi, K.; Venkatachalapathy, B.; Kaviya, M.; Mubeena, S.; Punnoose, A.M.; Sridhar, T.M. 6-O-tritylchitosan reinforced polycaprolactone nano scaffolds for bone replacement applications—a physicochemical study. *Mater. Res. Express* **2019**, *6*, 065308. [[CrossRef](#)]
123. Hu, W.-W.; Lin, C.-H.; Hong, Z.-J. The enrichment of cancer stem cells using composite alginate/polycaprolactone nanofibers. *Carbohydr. Polym.* **2019**, *206*, 70–79. [[CrossRef](#)]
124. Hou, J.; Wang, Y.; Xue, H.; Dou, Y. Biomimetic Growth of Hydroxyapatite on Electrospun CA/PVP Core–Shell Nanofiber Membranes. *Polymers* **2018**, *10*, 1032. [[CrossRef](#)]
125. Sharifi, F.; Atyabi, S.M.; Norouzi, D.; Zandi, M.; Irani, S.; Bakhshi, H. Polycaprolactone/carboxymethyl chitosan nanofibrous scaffolds for bone tissue engineering application. *Int. J. Biol. Macromol.* **2018**, *115*, 243–248. [[CrossRef](#)]
126. Shrestha, B.K.; Mousa, H.M.; Tiwari, A.P.; Ko, S.W.; Park, C.H.; Kim, C.S. Development of polyamide-6,6/chitosan electrospun hybrid nanofibrous scaffolds for tissue engineering application. *Carbohydr. Polym.* **2016**, *148*, 107–114. [[CrossRef](#)]
127. Sadeghi, D.; Karbasi, S.; Razavi, S.; Mohammadi, S.; Shokrgozar, M.A.; Bonakdar, S. Electrospun poly (hydroxybutyrate)/chitosan blend fibrous scaffolds for cartilage tissue engineering. *J. Appl. Polym. Sci.* **2016**, *133*, 9. [[CrossRef](#)]
128. Agrawal, P.; Pramanik, K. Chitosan-poly (vinyl alcohol) nanofibers by free surface electrospinning for tissue engineering applications. *Tissue Eng. Regen. Med.* **2016**, *13*, 485–497. [[CrossRef](#)]
129. Li, H.; Ding, Q.; Chen, X.; Huang, C.; Jin, X.; Ke, Q. A facile method for fabricating nano/microfibrous three-dimensional scaffold with hierarchically porous to enhance cell infiltration. *J. Appl. Polym. Sci.* **2019**, *136*, 47046. [[CrossRef](#)]

130. Fadaie, M.; Mirzaei, E.; Geramizadeh, B.; Asvar, Z. Incorporation of nanofibrillated chitosan into electrospun PCL nanofibers makes scaffolds with enhanced mechanical and biological properties. *Carbohydr. Polym.* **2018**, *199*, 628–640. [[CrossRef](#)]
131. Huang, M.; Li, J.; Chen, J.; Zhou, M.; He, J. Preparation of CS/PVA Nanofibrous Membrane with Tunable Mechanical Properties for Tympanic Member Repair. *Macromol. Res.* **2018**, *26*, 892–899. [[CrossRef](#)]
132. Thomas, M.S.; Pillai, P.K.S.; Faria, M.; Cordeiro, N.; Barud, H.; Thomas, S.; Pothan, L.A. Electrospun polylactic acid-chitosan composite: A bio-based alternative for inorganic composites for advanced application. *J. Mater. Sci. Mater. Med.* **2018**, *29*, 137. [[CrossRef](#)]
133. Chanda, A.; Adhikari, J.; Ghosh, A.; Chowdhury, S.R.; Thomas, S.; Datta, P.; Saha, P. Electrospun chitosan/polycaprolactone-hyaluronic acid bilayered scaffold for potential wound healing applications. *Int. J. Biol. Macromol.* **2018**, *116*, 774–785. [[CrossRef](#)]
134. Mohamadi, F.; Ebrahimi-Barough, S.; Reza Nourani, M.; Ali Derakhshan, M.; Goodarzi, V.; Sadegh Nazockdast, M.; Farokhi, M.; Tajerian, R.; Faridi Majidi, R.; Ai, J. Electrospun nerve guide scaffold of poly (ϵ -caprolactone)/collagen/nanobioglass: An In Vitro study in peripheral nerve tissue engineering. *J. Biomed. Mater. Res. Part A* **2017**, *105*, 1960–1972. [[CrossRef](#)]
135. Kang, Y.; Chen, P.; Shi, X.; Zhang, G.; Wang, C. Multilevel structural stereocomplex polylactic acid/collagen membranes by pattern electrospinning for tissue engineering. *Polymer* **2018**, *156*, 250–260. [[CrossRef](#)]
136. Park, H.K.; Joo, W.; Gu, B.K.; Ha, M.Y.; You, S.J.; Chun, H.J. Collagen/poly (d,l-lactic-co-glycolic acid) composite fibrous scaffold prepared by independent nozzle control multi-electrospinning apparatus for dura repair. *J. Ind. Eng. Chem.* **2018**, *66*, 430–437. [[CrossRef](#)]
137. Kim, J.I.; Kim, C.S. Harnessing nanotopography of PCL/collagen nanocomposite membrane and changes in cell morphology coordinated with wound healing activity. *Mater. Sci. Eng. C* **2018**, *91*, 824–837. [[CrossRef](#)]
138. Middleton, R.; Li, X.; Shepherd, J.; Li, Z.; Wang, W.; Best, S.M.; Cameron, R.E.; Huang, Y.Y.S. Near-Field Electrospinning Patterning Polycaprolactone and Polycaprolactone/Collagen Interconnected Fiber Membrane. *Macromol. Mater. Eng.* **2018**, *303*, 1700463. [[CrossRef](#)]
139. Gao, S.; Chen, M.; Wang, P.; Li, Y.; Yuan, Z.; Guo, W.; Zhang, Z.; Zhang, X.; Jing, X.; Li, X.; et al. An electrospun fiber reinforced scaffold promotes total meniscus regeneration in rabbit meniscectomy model. *Acta Biomater.* **2018**, *73*, 127–140. [[CrossRef](#)]
140. Gao, S.; Guo, W.; Chen, M.; Yuan, Z.; Wang, M.; Zhang, Y.; Liu, S.; Xi, T.; Guo, Q. Fabrication and characterization of electrospun nanofibers composed of decellularized meniscus extracellular matrix and polycaprolactone for meniscus tissue engineering. *J. Mater. Chem. B* **2017**, *5*, 2273–2285. [[CrossRef](#)]
141. Chen, Y.; Ye, S.-H.; Sato, H.; Zhu, Y.; Shanov, V.; Tiasa, T.; D'Amore, A.; Luketich, S.; Wan, G.; Wagner, W.R. Hybrid scaffolds of Mg alloy mesh reinforced polymer/extracellular matrix composite for critical-sized calvarial defect reconstruction. *J. Tissue Eng. Regen. Med.* **2018**, *12*, 1374–1388. [[CrossRef](#)]
142. Saadatkish, N.; Nouri Khorasani, S.; Morshed, M.; Allafchian, A.-R.; Beigi, M.-H.; Masoudi Rad, M.; Esmaeely Neisiany, R.; Nasr-Esfahani, M.-H. A ternary nanofibrous scaffold potential for central nerve system tissue engineering. *J. Biomed. Mater. Res. Part A* **2018**, *106*, 2394–2401. [[CrossRef](#)]
143. Hu, J.; Kai, D.; Ye, H.; Tian, L.; Ding, X.; Ramakrishna, S.; Loh, X.J. Electrospinning of poly (glycerol sebacate)-based nanofibers for nerve tissue engineering. *Mater. Sci. Eng. C* **2017**, *70*, 1089–1094. [[CrossRef](#)] [[PubMed](#)]
144. Jiang, Y.-C.; Jiang, L.; Huang, A.; Wang, X.-F.; Li, Q.; Turng, L.-S. Electrospun polycaprolactone/gelatin composites with enhanced cell-matrix interactions as blood vessel endothelial layer scaffolds. *Mater. Sci. Eng. C* **2017**, *71*, 901–908. [[CrossRef](#)] [[PubMed](#)]
145. Kook, Y.-M.; Kim, H.; Kim, S.; Heo, C.Y.; Park, M.H.; Lee, K.; Koh, W.-G. Promotion of Vascular Morphogenesis of Endothelial Cells Co-Cultured with Human Adipose-Derived Mesenchymal Stem Cells Using Polycaprolactone/Gelatin Nanofibrous Scaffolds. *Nanomaterials* **2018**, *8*, 117. [[CrossRef](#)] [[PubMed](#)]
146. Yu, K.; Zhou, X.; Zhu, T.; Wu, T.; Wang, J.; Fang, J.; El-Aassar, M.R.; El-Hamshary, H.; El-Newehy, M.; Mo, X. Fabrication of poly (ester-urethane)urea elastomer/gelatin electrospun nanofibrous membranes for potential applications in skin tissue engineering. *Rsc Adv.* **2016**, *6*, 73636–73644. [[CrossRef](#)]
147. Ma, J.; He, Y.; Liu, X.; Chen, W.; Wang, A.; Lin, C.-Y.; Mo, X.; Ye, X. A novel electrospun-aligned nanoyarn/three-dimensional porous nanofibrous hybrid scaffold for annulus fibrosus tissue engineering. *Int. J. Nanomed.* **2018**, *13*, 1553–1567. [[CrossRef](#)] [[PubMed](#)]

148. Baghersad, S.; Hajir Bahrami, S.; Mohammadi, M.R.; Mojtahedi, M.R.M.; Milan, P.B. Development of biodegradable electrospun gelatin/aloe-vera/poly (ϵ -caprolactone) hybrid nanofibrous scaffold for application as skin substitutes. *Mater. Sci. Eng. C* **2018**, *93*, 367–379. [\[CrossRef\]](#)
149. Saravani, S.; Ebrahimian-Hosseiniabadi, M.; Mohebbi-Kalhor, D. Polyglycerol sebacate/chitosan/gelatin nano-composite scaffolds for engineering neural construct. *Mater. Chem. Phys.* **2019**, *222*, 147–151. [\[CrossRef\]](#)
150. Sadeghi, A.; Pezeshki-Modaress, M.; Zandi, M. Electrospun polyvinyl alcohol/gelatin/chondroitin sulfate nanofibrous scaffold: Fabrication and In Vitro evaluation. *Int. J. Biol. Macromol.* **2018**, *114*, 1248–1256. [\[CrossRef\]](#)
151. Ye, K.; Liu, D.; Kuang, H.; Cai, J.; Chen, W.; Sun, B.; Xia, L.; Fang, B.; Morsi, Y.; Mo, X. Three-dimensional electrospun nanofibrous scaffolds displaying bone morphogenetic protein-2-derived peptides for the promotion of osteogenic differentiation of stem cells and bone regeneration. *J. Colloid Interface Sci.* **2019**, *534*, 625–636. [\[CrossRef\]](#)
152. Chen, W.; Chen, S.; Morsi, Y.; El-Hamshary, H.; El-Newhy, M.; Fan, C.; Mo, X. Superabsorbent 3D Scaffold Based on Electrospun Nanofibers for Cartilage Tissue Engineering. *ACS Appl. Mater. Interfaces* **2016**, *8*, 24415–24425. [\[CrossRef\]](#)
153. Zhao, Q.; Cui, H.; Wang, J.; Chen, H.; Wang, Y.; Zhang, L.; Du, X.; Wang, M. Regulation Effects of Biomimetic Hybrid Scaffolds on Vascular Endothelium Remodeling. *ACS Appl. Mater. Interfaces* **2018**, *10*, 23583–23594. [\[CrossRef\]](#)
154. Zhao, Q.; Wang, J.; Cui, H.; Chen, H.; Wang, Y.; Du, X. Programmed Shape-Morphing Scaffolds Enabling Facile 3D Endothelialization. *Adv. Funct. Mater.* **2018**, *28*, 1801027. [\[CrossRef\]](#)
155. Garcia Garcia, A.; Hébraud, A.; Duval, J.-L.; Wittmer, C.R.; Gaut, L.; Duprez, D.; Egles, C.; Bedoui, F.; Schlatter, G.; Legallais, C. Poly (ϵ -caprolactone)/Hydroxyapatite 3D Honeycomb Scaffolds for a Cellular Microenvironment Adapted to Maxillofacial Bone Reconstruction. *ACS Biomater. Sci. Eng.* **2018**, *4*, 3317–3326. [\[CrossRef\]](#)
156. Prabha, R.D.; Kraft, D.C.E.; Harkness, L.; Melsen, B.; Varma, H.; Nair, P.D.; Kjem, J.; Kassem, M. Bioactive nano-fibrous scaffold for vascularized craniofacial bone regeneration. *J. Tissue Eng. Regen. Med.* **2018**, *12*, e1537–e1548. [\[CrossRef\]](#)
157. Tiwari, A.P.; Joshi, M.K.; Kim, J.I.; Unnithan, A.R.; Lee, J.; Park, C.H.; Kim, C.S. Bimodal fibrous structures for tissue engineering: Fabrication, characterization and In Vitro biocompatibility. *J. Colloid Interface Sci.* **2016**, *476*, 29–34. [\[CrossRef\]](#)
158. Grant, R.; Hallett, J.; Forbes, S.; Hay, D.; Callanan, A. Blended electrospinning with human liver extracellular matrix for engineering new hepatic microenvironments. *Sci. Rep.* **2019**, *9*, 6293. [\[CrossRef\]](#)
159. Kim, J.Y.; Kim, J.I.; Park, C.H.; Kim, C.S. Design of a modified electrospinning for the in-situ fabrication of 3D cotton-like collagen fiber bundle mimetic scaffold. *Mater. Lett.* **2019**, *236*, 521–525. [\[CrossRef\]](#)
160. Song, S.J.; Shin, Y.C.; Kim, S.E.; Kwon, I.K.; Lee, J.H.; Hyon, S.H.; Han, D.W.; Kim, B. Aligned laminin core-polydioxanone/collagen shell fiber matrices effective for neuritogenesis. *Sci. Rep.* **2018**, *8*, 11. [\[CrossRef\]](#)
161. Liu, X.; Zhou, L.; Heng, P.; Xiao, J.; Lv, J.; Zhang, Q.; Hickey, M.E.; Tu, Q.; Wang, J. Lecithin doped electrospun poly(lactic acid)-thermoplastic polyurethane fibers for hepatocyte viability improvement. *Colloids Surf. B Biointerfaces* **2019**, *175*, 264–271. [\[CrossRef\]](#)
162. Wang, J.; Tian, L.; Luo, B.; Ramakrishna, S.; Kai, D.; Loh, X.J.; Yang, I.H.; Deen, G.R.; Mo, X. Engineering PCL/lignin nanofibers as an antioxidant scaffold for the growth of neuron and Schwann cell. *Colloids Surf. B Biointerfaces* **2018**, *169*, 356–365. [\[CrossRef\]](#)
163. Jaganathan, S.K.; Mani, M.P.; Palaniappan, S.K.; Rathanasamy, R. Fabrication and characterisation of nanofibrous polyurethane scaffold incorporated with corn and neem oil using single stage electrospinning technique for bone tissue engineering applications. *J. Polym. Res.* **2018**, *25*, 146. [\[CrossRef\]](#)
164. Didekhani, R.; Sohrabi, M.R.; Seyedjafari, E.; Soleimani, M.; Hanaee-Ahvaz, H. Electrospun composite PLLA/Oyster shell scaffold enhances proliferation and osteogenic differentiation of stem cells. *Biologicals* **2018**, *54*, 33–38. [\[CrossRef\]](#)
165. Du, J.; Zhu, T.; Yu, H.; Zhu, J.; Sun, C.; Wang, J.; Chen, S.; Wang, J.; Guo, X. Potential applications of three-dimensional structure of silk fibroin/poly (ester-urethane) urea nanofibrous scaffold in heart valve tissue engineering. *Appl. Surf. Sci.* **2018**, *447*, 269–278. [\[CrossRef\]](#)
166. Zhu, C.H.; Zhu, J.H.; Wang, C.W.; Chen, R.H.; Sun, L.N.; Ru, C.H. Wrinkle-Free, Sandwich, Electrospun PLGA/SF Nanofibrous Scaffold for Skin Tissue Engineering. *IEEE Trans. Nanotechnol.* **2018**, *17*, 675–679. [\[CrossRef\]](#)

167. Yi, B.; Zhang, H.; Yu, Z.; Yuan, H.; Wang, X.; Zhang, Y. Fabrication of high performance silk fibroin fibers via stable jet electrospinning for potential use in anisotropic tissue regeneration. *J. Mater. Chem. B* **2018**, *6*, 3934–3945. [[CrossRef](#)]
168. Luo, J.; Zhang, H.; Zhu, J.; Cui, X.; Gao, J.; Wang, X.; Xiong, J. 3-D mineralized silk fibroin/polycaprolactone composite scaffold modified with polyglutamate conjugated with BMP-2 peptide for bone tissue engineering. *Colloids Surf. B Biointerfaces* **2018**, *163*, 369–378. [[CrossRef](#)]
169. Cai, J.; Wang, J.; Ye, K.; Li, D.; Ai, C.; Sheng, D.; Jin, W.; Liu, X.; Zhi, Y.; Jiang, J.; et al. Dual-layer aligned-random nanofibrous scaffolds for improving gradient microstructure of tendon-to-bone healing in a rabbit extra-articular model. *Int. J. Nanomed.* **2018**, *13*, 3481–3492. [[CrossRef](#)]
170. Yao, Q.K.; Hu, Y.; Yu, F.; Zhang, W.J.; Fu, Y. A novel application of electrospun silk fibroin/poly (l-lactic acid-co-epsilon-caprolactone) scaffolds for conjunctiva reconstruction. *RSC Adv.* **2018**, *8*, 18372–18380. [[CrossRef](#)]
171. Serôdio, R.; Schickert, S.L.; Costa-Pinto, A.R.; Dias, J.R.; Granja, P.L.; Yang, F.; Oliveira, A.L. Ultrasound sonication prior to electrospinning tailors silk fibroin/PEO membranes for periodontal regeneration. *Mater. Sci. Eng. C* **2019**, *98*, 969–981. [[CrossRef](#)]
172. Cheng, G.; Ma, X.; Li, J.; Cheng, Y.; Cao, Y.; Wang, Z.; Shi, X.; Du, Y.; Deng, H.; Li, Z. Incorporating platelet-rich plasma into coaxial electrospun nanofibers for bone tissue engineering. *Int. J. Pharm.* **2018**, *547*, 656–666. [[CrossRef](#)]
173. Waghmare, V.S.; Wadke, P.R.; Dyawanapelly, S.; Deshpande, A.; Jain, R.; Dandekar, P. Starch based nanofibrous scaffolds for wound healing applications. *Bioact. Mater.* **2018**, *3*, 255–266. [[CrossRef](#)]
174. Jaganathan, S.K.; Mani, M.P.; Nageswaran, G.; Krishnasamy, N.P.; Ayyar, M. Single stage electrospun multicomponent scaffold for bone tissue engineering application. *Polym. Test.* **2018**, *70*, 244–254. [[CrossRef](#)]
175. He, J.; Zhou, Y.; Qi, K.; Wang, L.; Li, P.; Cui, S. Continuous twisted nanofiber yarns fabricated by double conjugate electrospinning. *Fibers Polym.* **2013**, *14*, 1857–1863. [[CrossRef](#)]
176. Gao, Y.; Shao, W.; Qian, W.; He, J.; Zhou, Y.; Qi, K.; Wang, L.; Cui, S.; Wang, R. Biom mineralized poly (l-lactic-co-glycolic acid)-tussah silk fibroin nanofiber fabric with hierarchical architecture as a scaffold for bone tissue engineering. *Mater. Sci. Eng. C* **2018**, *84*, 195–207. [[CrossRef](#)]
177. Jaganathan, S.K.; Fauzi Ismail, A. Production and hemocompatibility assessment of novel electrospun polyurethane nanofibers loaded with dietary virgin coconut oil for vascular graft applications. *J. Bioact. Compat. Polym.* **2017**, *33*, 210–223. [[CrossRef](#)]
178. Pedram Rad, Z.; Mokhtari, J.; Abbasi, M. Fabrication and characterization of PCL/zein/gum arabic electrospun nanocomposite scaffold for skin tissue engineering. *Mater. Sci. Eng. C* **2018**, *93*, 356–366. [[CrossRef](#)]
179. Zakaria, S.M.; Sharif, S.H.; Othman, M.R.; Yang, F.; Jansen, J.A. Nanophase Hydroxyapatite as a Biomaterial in Advanced Hard Tissue Engineering: A Review. *Tissue Eng. Part B-Rev.* **2013**, *19*, 431–441. [[CrossRef](#)]
180. Shin, S.R.; Li, Y.C.; Jang, H.L.; Khoshakhlagh, P.; Akbari, M.; Nasajpour, A.; Zhang, Y.S.; Tamayol, A.; Khademhosseini, A. Graphene-based materials for tissue engineering. *Adv. Drug Deliv. Rev.* **2016**, *105*, 255–274. [[CrossRef](#)]
181. Ito, A.; Kamihira, M. Tissue Engineering Using Magnetite Nanoparticles. In *Nanoparticles in Translational Science and Medicine*; Villaverde, A., Ed.; Elsevier Academic Press Inc.: San Diego, CA, USA, 2011; Volume 104, pp. 355–395.
182. Cardoso, V.F.; Francesko, A.; Ribeiro, C.; Banobre-Lopez, M.; Martins, P.; Lanceros-Mendez, S. Advances in Magnetic Nanoparticles for Biomedical Applications. *Adv. Healthc. Mater.* **2018**, *7*, 35. [[CrossRef](#)]
183. Sedghi, R.; Sayyari, N.; Shaabani, A.; Niknejad, H.; Tayebi, T. Novel biocompatible zinc-curcumin loaded coaxial nanofibers for bone tissue engineering application. *Polymer* **2018**, *142*, 244–255. [[CrossRef](#)]
184. Xu, Z.; Zhao, R.; Huang, X.; Wang, X.; Tang, S. Fabrication and biocompatibility of agarose acetate nanofibrous membrane by electrospinning. *Carbohydr. Polym.* **2018**, *197*, 237–245. [[CrossRef](#)]
185. Golafshan, N.; Kharaziha, M.; Fathi, M. Tough and conductive hybrid graphene-PVA: Alginate fibrous scaffolds for engineering neural construct. *Carbon* **2017**, *111*, 752–763. [[CrossRef](#)]
186. Shrestha, S.; Shrestha, B.K.; Kim, J.I.; Won Ko, S.; Park, C.H.; Kim, C.S. Electroless coating polypyrrole on chitosan grafted polyurethane with functionalized multiwall carbon nanotubes electrospun scaffold for nerve tissue engineering. *Carbon* **2018**, *136*, 430–443. [[CrossRef](#)]
187. Mahmoudi, N.; Simchi, A. On the biological performance of graphene oxide-modified chitosan/polyvinyl pyrrolidone nanocomposite membranes: In Vitro and In Vivo effects of graphene oxide. *Mater. Sci. Eng. C* **2017**, *70*, 121–131. [[CrossRef](#)]

188. Nasajpour, A.; Ansari, S.; Rinoldi, C.; Rad, A.S.; Aghaloo, T.; Shin, S.R.; Mishra, Y.K.; Adelung, R.; Swieszkowski, W.; Annabi, N.; et al. A Multifunctional Polymeric Periodontal Membrane with Osteogenic and Antibacterial Characteristics. *Adv. Funct. Mater.* **2018**, *28*, 1703437. [\[CrossRef\]](#)
189. Li, H.; Huang, C.; Jin, X.; Ke, Q. An electrospun poly (ϵ -caprolactone) nanocomposite fibrous mat with a high content of hydroxyapatite to promote cell infiltration. *RSC Adv.* **2018**, *8*, 25228–25235. [\[CrossRef\]](#)
190. Wu, G.; Deng, X.; Song, J.; Chen, F. Enhanced biological properties of biomimetic apatite fabricated polycaprolactone/chitosan nanofibrous bio-composite for tendon and ligament regeneration. *J. Photochem. Photobiol. B Biol.* **2018**, *178*, 27–32. [\[CrossRef\]](#)
191. Pavličáková, V.; Fohlerová, Z.; Pavličák, D.; Khunová, V.; Vojtová, L. Effect of halloysite nanotube structure on physical, chemical, structural and biological properties of elastic polycaprolactone/gelatin nanofibers for wound healing applications. *Mater. Sci. Eng. C* **2018**, *91*, 94–102. [\[CrossRef\]](#)
192. Guo, F.; Zhang, H.; Qiu, G.; Zuo, H.; Chen, G.; Lou, Y.; Min, D.; Guo, G. Fabrication of LaCl₃-containing nanofiber scaffolds and their application in skin wound healing. *J. Appl. Polym. Sci.* **2018**, *135*, 46672. [\[CrossRef\]](#)
193. Ezati, M.; Safavipour, H.; Houshmand, B.; Faghihi, S. Development of a PCL/gelatin/chitosan/ β -TCP electrospun composite for guided bone regeneration. *Prog. Biomater.* **2018**, *7*, 225–237. [\[CrossRef\]](#)
194. Thompson, Z.; Rahman, S.; Yarmolenko, S.; Sankar, J.; Kumar, D.; Bhattarai, N. Fabrication and Characterization of Magnesium Ferrite-Based PCL/Aloe Vera Nanofibers. *Materials* **2017**, *10*, 937. [\[CrossRef\]](#)
195. Rijal, N.P.; Adhikari, U.; Khanal, S.; Pai, D.; Sankar, J.; Bhattarai, N. Magnesium oxide-poly (ϵ -caprolactone)-chitosan-based composite nanofiber for tissue engineering applications. *Mater. Sci. Eng. B* **2018**, *228*, 18–27. [\[CrossRef\]](#)
196. Stone, H.; Lin, S.; Mequanint, K. Preparation and characterization of electrospun rGO-poly (ester amide) conductive scaffolds. *Mater. Sci. Eng. C* **2019**, *98*, 324–332. [\[CrossRef\]](#)
197. Gorodzha, S.N.; Muslimov, A.R.; Syromotina, D.S.; Timin, A.S.; Tsvetkov, N.Y.; Lepik, K.V.; Petrova, A.V.; Surmeneva, M.A.; Gorin, D.A.; Sukhorukov, G.B.; et al. A comparison study between electrospun polycaprolactone and piezoelectric poly (3-hydroxybutyrate-co-3-hydroxyvalerate) scaffolds for bone tissue engineering. *Colloids Surf. B Biointerfaces* **2017**, *160*, 48–59. [\[CrossRef\]](#)
198. Ramesh, S.; Lungaro, L.; Tsikritsis, D.; Weflen, E.; Rivero, I.V.; Elfick, A.P.D. Fabrication and evaluation of poly (lactic acid), chitosan, and tricalcium phosphate biocomposites for guided bone regeneration. *J. Appl. Polym. Sci.* **2018**, *135*, 46692. [\[CrossRef\]](#)
199. Sabzi, M.; Ranjbar-Mohammadi, M.; Zhang, Q.; Kargozar, S.; Leng, J.; Akhtari, T.; Abbasi, R. Designing triple-shape memory polymers from a miscible polymer pair through dual-electrospinning technique. *J. Appl. Polym. Sci.* **2019**, *136*, 47471. [\[CrossRef\]](#)
200. Shin, Y.C.; Lee, J.H.; Jin, L.; Kim, M.J.; Kim, Y.-J.; Hyun, J.K.; Jung, T.-G.; Hong, S.W.; Han, D.-W. Stimulated myoblast differentiation on graphene oxide-impregnated PLGA-collagen hybrid fibre matrices. *J. Nanobiotechnology* **2015**, *13*, 21. [\[CrossRef\]](#)
201. Yang, X.; Li, Y.Y.; Liu, X.J.; Huang, Q.L.; Zhang, R.R.; Feng, Q.L. Incorporation of silica nanoparticles to PLGA electrospun fibers for osteogenic differentiation of human osteoblast-like cells. *Regen. Biomater.* **2018**, *5*, 229–238. [\[CrossRef\]](#)
202. Lai, W.-Y.; Feng, S.-W.; Chan, Y.-H.; Chang, W.-J.; Wang, H.-T.; Huang, H.-M. In Vivo Investigation into Effectiveness of Fe₃O₄/PLLA Nanofibers for Bone Tissue Engineering Applications. *Polymers* **2018**, *10*, 804. [\[CrossRef\]](#)
203. Lee, S.; Joshi, M.K.; Tiwari, A.P.; Maharjan, B.; Kim, K.S.; Yun, Y.-H.; Park, C.H.; Kim, C.S. Lactic acid assisted fabrication of bioactive three-dimensional PLLA/ β -TCP fibrous scaffold for biomedical application. *Chem. Eng. J.* **2018**, *347*, 771–781. [\[CrossRef\]](#)
204. Zhou, T.; Li, G.; Lin, S.; Tian, T.; Ma, Q.; Zhang, Q.; Shi, S.; Xue, C.; Ma, W.; Cai, X.; et al. Electrospun Poly (3-hydroxybutyrate-co-4-hydroxybutyrate)/Graphene Oxide Scaffold: Enhanced Properties and Promoted in Vivo Bone Repair in Rats. *ACS Appl. Mater. Interfaces* **2017**, *9*, 42589–42600. [\[CrossRef\]](#)
205. Jaganathan, S.K.; Mani, M.P. Single-stage synthesis of electrospun polyurethane scaffold impregnated with zinc nitrate nanofibers for wound healing applications. *J. Appl. Polym. Sci.* **2019**, *136*, 46942. [\[CrossRef\]](#)
206. Drupitha, M.P.; Das, B.; Parameswaran, R.; Dhara, S.; Nando, G.B.; Naskar, K. Hybrid electrospun fibers based on TPU-PDMS and spherical nanohydroxyapatite for bone tissue engineering. *Mater. Today Commun.* **2018**, *16*, 264–273. [\[CrossRef\]](#)

207. Enayati, M.S.; Behzad, T.; Sajkiewicz, P.; Rafienia, M.; Bagheri, R.; Ghasemi-Mobarakeh, L.; Kolbuk, D.; Pahlevanneshan, Z.; Bonakdar, S.H. Development of electrospun poly (vinyl alcohol)-based bionanocomposite scaffolds for bone tissue engineering. *J. Biomed. Mater. Res. Part A* **2018**, *106*, 1111–1120. [\[CrossRef\]](#)
208. Ngadiman, H.N.; Yusof, M.N.; Idris, A.; Fallahiarezoudar, E.; Kurniawan, D. Novel Processing Technique to Produce Three Dimensional Polyvinyl Alcohol/Maghemite Nanofiber Scaffold Suitable for Hard Tissues. *Polymers* **2018**, *10*, 353. [\[CrossRef\]](#)
209. Kim, J.I.; Lee, J.C.; Kim, M.J.; Park, C.H.; Kim, C.S. The impact of humidity on the generation and morphology of the 3D cotton-like nanofibrous piezoelectric scaffold via an electrospinning method. *Mater. Lett.* **2019**, *236*, 510–513. [\[CrossRef\]](#)
210. Saburi, E.; Islami, M.; Hosseinzadeh, S.; Moghadam, A.S.; Mansour, R.N.; Azadian, E.; Joneidi, Z.; Nikpoor, A.R.; Ghadiani, M.H.; Khodaii, Z.; et al. In Vitro osteogenic differentiation potential of the human induced pluripotent stem cells augments when grown on Graphene oxide-modified nanofibers. *Gene* **2019**, *696*, 72–79. [\[CrossRef\]](#)
211. Nalvuran, H.; Elçin, A.E.; Elçin, Y.M. Nanofibrous silk fibroin/reduced graphene oxide scaffolds for tissue engineering and cell culture applications. *Int. J. Biol. Macromol.* **2018**, *114*, 77–84. [\[CrossRef\]](#)
212. Brito-Pereira, R.; Correia, D.M.; Ribeiro, C.; Francesko, A.; Etxebarria, I.; Pérez-Álvarez, L.; Vilas, J.L.; Martins, P.; Lanceros-Mendez, S. Silk fibroin-magnetic hybrid composite electrospun fibers for tissue engineering applications. *Compos. Part B Eng.* **2018**, *141*, 70–75. [\[CrossRef\]](#)
213. Wang, S.-D.; Ma, Q.; Wang, K.; Chen, H.-W. Improving Antibacterial Activity and Biocompatibility of Bioinspired Electrospinning Silk Fibroin Nanofibers Modified by Graphene Oxide. *ACS Omega* **2018**, *3*, 406–413. [\[CrossRef\]](#)
214. Koppes, A.N.; Zaccor, N.W.; Rivet, C.J.; Williams, L.A.; Piselli, J.M.; Gilbert, R.J.; Thompson, D.M. Neurite outgrowth on electrospun PLLA fibers is enhanced by exogenous electrical stimulation. *J. Neural Eng.* **2014**, *11*, 046002. [\[CrossRef\]](#)
215. Fuh, Y.-K.; Wu, Y.-C.; He, Z.-Y.; Huang, Z.-M.; Hu, W.-W. The control of cell orientation using biodegradable alginate fibers fabricated by near-field electrospinning. *Mater. Sci. Eng.* **2016**, *62*, 879–887. [\[CrossRef\]](#)



© 2019 by the authors. Licensee MDPI, Basel, Switzerland. This article is an open access article distributed under the terms and conditions of the Creative Commons Attribution (CC BY) license (<http://creativecommons.org/licenses/by/4.0/>).